Long non-coding RNA repertoire and targeting by nuclear exosome, cytoplasmic exonuclease and RNAi in fission yeast

Sophie R Atkinson[1*], Samuel Marguerat[1,2,3*], Danny A Bitton[1*], Maria Rodríguez-López[1],

Charalampos Rallis[1,7], Jean-François Lemay[4], Cristina Cotobal[1], Michal Malecki[1],

Pawel Smialowski[5], Juan Mata[6], Philipp Korber[5], François Bachand[4], Jürg Bähler[1+]

[1] University College London, Research Department of Genetics, Evolution & Environment and UCL Genetics Institute, London, WC1E 6BT, UK.

[2] MRC London Institute of Medical Sciences (LMS), London W12 0NN UK

[3] Institute of Clinical Sciences (ICS), Faculty of Medicine, Imperial College London, London W12 0NN UK

[4] Université de Sherbrooke, Department of Biochemistry, Sherbrooke, Quebec J1H 5N4, Canada.

[5] LMU Munich, Biomedical Center, 82152 Planegg-Martinsried near Munich, Germany.

[6] Department of Biochemistry, University of Cambridge, Cambridge CB2 1QW, UK.

[7] Current address: University of East London, School of Health Sports and Bioscience, London, EN15 4LZ, London, UK.

* Equal contributions.

[+] Correspondence: Email: j.bahler@ucl.ac.uk

Address: Prof. Jürg Bähler, University College London, Gower Street,

Darwin Building – GEE, London WC1E 6BT, United Kingdom

Phone: +44(0)203-108-1602

Running title: Long non-coding RNAs in fission yeast

Keywords: pervasive transcription, NMD pathway, Schizosaccharomyces pombe, RNA degradation, antisense RNA, cytoplasmic exonuclease.

ABSTRACT

Long non-coding RNAs (lncRNAs), which are longer than 200 nucleotides but often

unstable, contribute a substantial and diverse portion to pervasive non-coding

transcriptomes. Most lncRNAs are poorly annotated and understood, although several play

important roles in gene regulation and diseases. Here we systematically uncover and

analyse lncRNAs in *Schizosaccharomyces pombe.* Based on RNA-seq data from twelve

RNA-processing mutants and nine physiological conditions, we identify 5775 novel lncRNAs,

nearly 4-times the previously annotated lncRNAs. The expression of most lncRNAs

becomes strongly induced under the genetic and physiological perturbations, most notably

during late meiosis. Most lncRNAs are cryptic and suppressed by three RNA-processing

pathways: the nuclear exosome, cytoplasmic exonuclease, and RNAi. Double-mutant

analyses reveal substantial coordination and redundancy among these pathways. We

classify lncRNAs by their dominant pathway into cryptic unstable transcripts (CUTs), Xrn1-

sensitive unstable transcripts (XUTs), and Dicer-sensitive unstable transcripts (DUTs).

XUTs and DUTs are enriched for antisense lncRNAs, while CUTs are often bidirectional and

actively translated. The cytoplasmic exonuclease, along with RNAi, dampens the

expression of thousands of lncRNAs and mRNAs that become induced during meiosis.

Antisense lncRNA expression mostly negatively correlates with sense mRNA expression in

the physiological, but not the genetic conditions. Intergenic and bidirectional lncRNAs

emerge from nucleosome-depleted regions, upstream of positioned nucleosomes. Our

results highlight both similarities and differences to lncRNA regulation in budding yeast. This

broad survey of the lncRNA repertoire and characteristics in *S. pombe,* and the interwoven

regulatory pathways that target lncRNAs, provides a rich framework for their further

functional analyses.

INTRODUCTION

Genomes are more pervasively transcribed than expected from their protein-coding sequences. For example, over 80% of the human genome is transcribed but only ~2% encodes proteins (Hangauer et al. 2013). So-called long non-coding RNAs (lncRNAs), which exceed 200 nucleotides in length but lack long open reading frames, make up a substantial and diverse portion of the non-coding transcriptome. The functions, if any, of most lncRNAs are not known, although several have well-defined roles in gene regulation and other cellular processes, and are also implicated in diseases (Geisler and Coller 2013; Batista and Chang 2013; Mercer and Mattick 2013; Guttman and Rinn 2012; Rinn and Chang 2012; Jandura and Krause 2017). In several cases, the act of transcription rather than the lncRNA itself is functionally relevant (Ard et al. 2017). The lncRNAs are often lowly expressed but show more changes in expression levels between different tissues or conditions than do the protein-coding messenger RNAs (mRNAs) (Cabili et al. 2011; Derrien et al. 2012; Pauli et al. 2012; Hon et al. 2017). In general, lncRNAs are transcribed by RNA polymerase II and seem to be capped and polyadenylated (Cabili et al. 2011; Derrien et al. 2012; Guttman et al. 2009), although the patterns of transcription and RNA processing can radically differ between mRNAs and lncRNAs (Schlackow et al. 2017; Tuck and Tollervey 2013; Quinn and Chang 2016; Mukherjee et al. 2017). Some lncRNAs engage with ribosomes, which can trigger nonsense-mediated decay (NMD) to dampen their expression but may also produce functional peptides in some cases (de Andres-Pablo et al. 2017; Quinn and Chang 2016; Malabat et al. 2015; Wery et al. 2016).

Given the profusion, diversity and low expression of lncRNAs, their full description and annotation is still ongoing and evolving (Mattick and Rinn 2015; St. Laurent et al. 2015; Atkinson et al. 2012). A conceptually simple way to classify lncRNA genes is by their position relative to neighbouring coding genes. For example, long intervening non-coding RNAs (lincRNAs), transcribed from intergenic regions that do not overlap any mRNAs, have been the subject of much research in mammalian cells (Ulitsky and Bartel 2013; Rinn and Chang 2012; Schlackow et al. 2017). Antisense lncRNAs are transcribed in the opposite direction to mRNAs with which they completely or partially overlap; they can affect sense transcript levels via diverse mechanisms (Pelechano and

Steinmetz 2013; Mellor et al. 2016). Bidirectional lncRNAs, on the other hand, emerge close to the transcriptional start site of coding genes but run in the opposite direction; most eukaryotic promoters initiate divergent transcription leading to widespread bidirectional lncRNAs, although transcriptional elongation is often only productive in the sense direction (Quinn and Chang 2016; Grzechnik et al. 2014). Bidirectional transcription has been proposed to drive the origination of new genes (Wu and Sharp 2013) and modulate gene-expression noise (Wang et al. 2011).

Pervasive transcription is potentially harmful as it can affect the expression of coding genes (Mellor et al. 2016), and nascent RNAs can compromise genome stability (Li and Manley 2006). Cells therefore apply RNA surveillance systems to keep the expression of lncRNAs in check (Jensen et al. 2013). Many lncRNAs are actively degraded shortly after transcription, suggesting that they could reflect transcriptional noise, byproducts of coding transcription, or that the act of transcription, rather than the lncRNA itself, is functionally important (Jensen et al. 2013). Different RNA-decay pathways preferentially target distinct sets of lncRNAs, which has been used for lncRNA classification in budding yeast. The 'cryptic unstable transcripts' (CUTs) accumulate in cells lacking Rrp6 (Xu et al. 2009; Neil et al. 2009), a nuclear-specific catalytic subunit of the RNA exosome (Houseley and Tollervey 2009; Kilchert et al. 2016). Conversely, the 'stable unannotated transcripts' (SUTs) are less affected by Rrp6 (Xu et al. 2009; Neil et al. 2009). The human 'promoter upstream transcripts' (PROMPTs) are analogous to CUTs (Preker et al. 2008). The 'Xrn1-sensitive unstable transcripts' (XUTs) accumulate in cells lacking the cytoplasmic 5' exonuclease Xrn1 and are often antisense to mRNAs (van Dijk et al. 2011; Houseley and Tollervey 2009; Wery et al. 2018). 'Nrd1-unterminated transcripts' (NUTs) and 'Reb1p-dependent unstable transcripts' (RUTs) are controlled via different mechanisms of transcriptional termination linked to RNA degradation (Schulz et al. 2013; Colin et al. 2014). These classes, while useful, are somewhat arbitrary and overlapping as most lncRNAs can be targeted by different pathways, especially if one pathway is absent in mutant cells (Jensen et al. 2013).

The fission yeast *Schizosaccharomyces pombe* provides a potent complementary model system to study gene regulation. In some respects, RNA metabolism of fission yeast is more similar to metazoan cells than budding yeast. For example, RNA interference (RNAi) (Castel and Martienssen

2013), RNA uridylation (Schmidt et al. 2011), alternative-polyadenylation features (Liu et al. 2017), and Pab2/PABPN1-dependent RNA degradation (Lemay et al. 2010; Lemieux et al. 2011; Beaulieu et al. 2012) are conserved from fission yeast to humans, but not in budding yeast. Several genome-wide studies have uncovered widespread lncRNAs (Dutrow et al. 2008; Wilhelm et al. 2008; Rhind et al. 2011; Eser et al. 2016), and over 1500 lncRNAs are currently annotated in the PomBase model organism database (McDowall et al. 2014). Studies with natural isolates of *S. pombe* revealed that only the most highly expressed lncRNAs show purifying selection (Jeffares et al. 2015), but the regulation of many lncRNAs is affected by expression quantitative trait loci (Clément-Ziza et al. 2014). Over 85% of the annotated *S. pombe* lncRNAs are expressed below one copy per cell during proliferation, and over 97% appear to be polyadenylated (Marguerat et al. 2012). Ribosome profiling showed that as many as 24% of lncRNAs are actively translated (Duncan and Mata 2014). As in other organisms, a large proportion of the *S. pombe* lncRNAs are antisense to mRNAs and have been implicated in controlling the meiotic gene expression programme (Ni et al. 2010; Chen et al. 2012; Bitton et al. 2011; Wery et al. 2018). Diverse chromatin factors function in suppressing antisense and other lncRNAs in *S. pombe*, including the HIRA histone chaperone (Anderson et al. 2009), the histone variant H2A.Z (Zofall et al. 2009; Clément-Ziza et al. 2014), the Clr4/Suv39 methyltransferase together with RNAi (Zhang et al. 2011), the Spt6 histone chaperone (DeGennaro et al. 2013; Wery et al. 2018), and the CHD1 chromatin remodeller (Pointner et al. 2012; Hennig et al. 2012; Shim et al. 2012). Analogous to CUTs in budding yeast, different types of RNAs accumulating in *rrp6* mutants have also been described (Zhou et al. 2015). Several lncRNAs have been functionally characterized in *S. pombe*: *meiRNA* controls meiotic differentiation and chromosome pairing (Yamashita et al. 2016; Ding et al. 2012), stress-induced lncRNAs activate expression of the downstream *fbp1* gene during glucose starvation (Hirota et al. 2008; Oda et al. 2015), *adh1AS* is an antisense inhibitor of the *adh1* gene during zinc limitation (Ehrensberger et al. 2013), *prt* recruits the exosome to control phosphate-tuned *pho1* expression (Shah et al. 2014; Ard et al. 2014), *nc-tgp1* inhibits the phosphate-responsive permease *tgp1* gene by transcriptional interference (Ard et al. 2014), *nam1* regulates entry into meiotic differentiation (Touat‑Todeschini et al. 2017), and

SPNCRNA.1164 regulates expression of the *atf1* transcription-factor gene in *trans* during oxidative stress (Leong et al. 2014). Naturally, these studies only scratch the surface, with the non-coding transcriptome and any of its functions remaining relatively poorly defined in fission yeast and other organisms.

Transcriptome analyses under selective conditions, such as in RNA-processing mutants, have proven useful to define lncRNAs in budding yeast. Here we analyse transcriptome sequencing under multiple genetic and physiological perturbations in fission yeast to maximize the detection and initial characterization of lncRNAs. Some of these RNA-seq samples have previously been analysed with respect to mRNA processing and expression (Bitton et al. 2015a; Lemieux et al. 2011; Schlackow et al. 2013; Marguerat et al. 2012; Lemay et al. 2014). They interrogate pathways, such as RNAi and Pab2/PABPN1, which are conserved in humans but not in budding yeast. We identify 5775 novel, unannotated lncRNAs, in addition to the previously annotated lncRNAs. The expression of lncRNAs is more extensively regulated in stationary phase, quiescence and, most notably, meiotic differentiation than the expression of mRNAs. Many lncRNAs comprise unstable transcripts that are repressed by three partially overlapping RNA-processing pathways. Analogous to budding yeast, we classify the unstable lncRNAs targeted by Rrp6, Dcr1 and Exo2 into CUTs, DUTs and XUTs, respectively. We further analyse the positions and expression of all novel and annotated lncRNAs with respect to neighbouring mRNAs, and other biological characteristics such as translation and nucleosome patterns. Both similarities and notable differences to lncRNAs in budding yeast are discussed. This extensive study provides a framework for functional characterization of lncRNAs in fission yeast and beyond.

RESULTS

Detection of novel lncRNAs

To broadly identify lncRNAs in fission yeast, we examined strand-specific RNA-seq data acquired under multiple genetic and physiological conditions. We analysed the transcriptomes of twelve RNA-

processing mutants to facilitate detection of RNAs that may be rapidly degraded (Supplemental Table

S1). This mutant panel affects proteins for key pathways of RNA processing and degradation: Rrp6, a

3'-5' exonuclease of the nuclear RNA exosome (Harigaya et al. 2006; Lemay et al. 2014); Dis3, a 3'-

5' exo/endonuclease of the core RNA exosome (Wang et al. 2008); Ago1 (Argonaute), Dcr1 (RNase

III-like Dicer) and Rdp1 (RNA-dependent RNA polymerase) of the RNAi pathway (Volpe et al.

2002); Exo2, a cytoplasmic 5' exonuclease (ortholog of XRN1) (Houseley and Tollervey 2009); Ski7,

a cytoplasmic cofactor which links the Ski complex to the exosome (Lemay et al. 2010); Cid14, a

polyA polymerase of the TRAMP complex which is a cofactor of the nuclear RNA exosome (Wang et

al. 2008); Pab2, a polyA-binding protein targeting RNAs to the nuclear exosome (PABPN1 ortholog)

(Lemieux et al. 2011); Pan2, a deadenylase of the Pan2–Pan3 complex (Wolf and Passmore 2014);

and Upf1, an ATP-dependent RNA helicase of the NMD pathway (Rodríguez-Gabriel et al. 2006).

We also analysed transcriptomes under nine physiological conditions to sample key cellular states

(Supplemental Table S2): two timepoints of stationary phase after glucose depletion (100 and 50%

cell viability); two timepoints of quiescence/cellular ageing (days 1 and 7 after nitrogen removal); and

five timepoints of meiotic differentiation (0 to 8 h after triggering meiosis).

We designed a simple segmentation heuristic to detect novel lncRNAs longer than 200

nucleotides, favouring sensitivity at the cost of specificity (Materials and methods). Applying this

approach to the RNA-seq data covering the genetic and physiological perturbations, we identified

5775 novel, unannotated lncRNAs in addition to the ~1550 previously annotated lncRNAs. We

assigned systematic names, *SPNCRNA.2000* to *SPNCRNA.7774*, to these novel lncRNAs

(Supplemental Table S3). Of these unannotated lncRNAs, 159 fully or partially overlapped on the

same strand with 167 of the 487 novel lncRNAs recently reported (Eser et al. 2016) (Supplemental

Table S4). On the other hand, 214 of these 487 lncRNAs could not be validated using our data

(Supplemental Table S4). In our samples, these 214 lncRNAs typically showed no sequencing signals

in the sense strand, but strong signals on the opposite strand for these regions (Materials and

methods).

Naturally, annotation of weakly expressed lncRNAs based on RNA-seq data, and especially the

locations of their TSS and TTS, is somewhat arbitrary and should be understood as an approximation.

Nevertheless, our data reveal many more *S. pombe* lncRNAs than have been previously recognized, and the broad annotations provide a resource for further studies. We defined three confidence classes for all annotated and novel lncRNAs, based on RPKM values from the sequenced samples (Materials and methods). This approach resulted in 2090 high-confidence lncRNAs (1064 annotated, 1026 novel), 5004 medium-confidence lncRNAs (452 annotated, 4552 novel), and 254 low-confidence lncRNAs (57 annotated, 197 novel). So most novel lncRNAs are medium-confidence, while most annotated lncRNAs are high-confidence using our criteria. Supplemental Table S5 provides the confidence class for all annotated and novel lncRNAs. Examples of novel lncRNAs are provided in a browser view in Supplemental Figure S1. This figure suggests that some lncRNAs might consist of transcribed regions encompassing several smaller RNAs or variable, condition-specific isoforms. To assess these complexities for specific lncRNAs, we also provide a web tool to view RNA-seq data for all lncRNAs and mRNAs in the different conditions (http://bahlerlab.info/ncViewer). Our data will also be included in a specific track of the JBrowse genome brower in PomBase.

The novel lncRNAs were generally shorter (mean 797 nt) than the annotated lncRNAs (mean 1233 nt) and mRNAs (mean 2148 nt) (Supplemental Figure S2a). While some sequence library protocols can generate spurious antisense RNAs (Perocchi et al. 2007), our protocol is resilient to this artefact as it relies on ligating two RNA oligonucleotides to fragmented mRNAs. We mostly analysed polyA-enriched samples, because almost all *S. pombe* lncRNAs are polyadenylated (Marguerat et al. 2012). As a control, we compared the data to samples depleted for ribosomal RNA (rRNA) in *rrp6Δ* and *exo2Δ* mutants, which confirmed that the great majority of lncRNAs are polyadenylated (Supplemental Figure S2b). We cannot exclude the possibility, however, that some non-polyadenylated lncRNAs are missing from our annotation.

None of the novel lncRNAs overlapped with mRNAs on the same strand using current PomBase annotations, and only 21 overlapped using CAGE (Li et al. 2015) and polyA data (Mata 2013), respectively, for transcription start and termination sites (Supplemental Table S5). Thus, the novel lncRNAs do not represent alternative transcription start or termination sites of known mRNAs. On the other hand, 3650 of 5138 protein-coding regions (71%) overlapped by at least 10 nucleotides with antisense lncRNAs, either annotated or novel. The 1461 (28.4%) of coding regions not

associated with antisense lncRNAs were enriched for the 20% shortest mRNAs ($p \sim 1.6e^{-16}$), including

those encoding ribosomal proteins ($p \sim 1.1e^{-5}$), as well as for several features associated with high

gene expression, including high mRNA levels ($p \sim 0.004$) (Pancaldi et al. 2010), stable mRNAs (p

$\sim 2.1e^{-9}$) (Hasan et al. 2014), and mRNAs that show high RNA polymerase II occupancy ($p \sim 2.4e^{-5}$)

and high ribosome density ($p \sim 1.2e^{-41}$) (Lackner et al. 2007). These enrichments suggest that highly

expressed genes are either protected from antisense transcripts or interfere with antisense

transcription.

Figure 1 shows the relative expression changes of all mRNAs, annotated lncRNAs and novel

lncRNAs in the genetic and physiological conditions. For all conditions, differential expression was

determined relative to three reference samples (exponentially proliferating wild-type and auxotrophic

control cells in minimal medium with supplements; Supplemental Table S2). This panel of reference

samples included different genetic markers and supplements used for the other conditions. Only 403

RNAs, including 184 novel lncRNAs, were differentially expressed between wild-type and

auxotrophic control cells grown in rich yeast extract (YE) medium compared to minimal media (>2-

fold change, p <0.05). Thus, the growth medium and auxtrophic markers only minimally affected

lncRNA expression. All differential expression data are available in Supplemental Table S3.

About 50% of the mRNAs were differentially expressed, both induced and repressed, in the

different physiological conditions, but much less so in the different genetic conditions (Figure 1A and

Figure 2). The mRNAs up-regulated in the exosome, *pab2*, and RNAi mutants were enriched for

Gene Ontology (GO) terms related to meiosis, consistent with reported roles of the corresponding

proteins in meiotic gene silencing (St-André et al. 2010; Yamanaka et al. 2010, 2013). Notably,

mRNAs up-regulated in the *exo2* mutant were strongly and specifically enriched for middle meiotic

genes (Mata et al. 2002).

Figure 1B and C show the expression of the previously annotated and novel lncRNAs,

respectively. Compared to mRNAs, much higher proportions and numbers of lncRNAs featured

strong differential expression, mostly induced, under the different genetic and physiological

conditions (Figure 1B,C and Figure 2). The following mutants led to the most pronounced effects on

lncRNA expression: nuclear exosome (*rrp6-ts, rrp6Δ, dis3-54*), RNAi (*ago1Δ, dcr1Δ, rdp1Δ*), and the

cytoplasmic exonuclease (*exo2Δ*). In nuclear exosome mutants, most lncRNAs were strongly

derepressed, in stark contrast to the mRNAs which showed a higher proportion of repressed

transcripts in this condition (Figure 2, Figure 3A). Many of the novel lncRNAs in particular were

also strongly derepressed in RNAi and *exo2* mutants and in meiotic cells (Figure 3A), most notably

during late meiotic stages (Mei 6-8h; Figure 1C and Figure 2). On the other hand, the novel lncRNAs

showed generally lower expression levels in both genetic and physiological conditions than the

annotated lncRNAs, and much lower than the mRNAs (Figure 3B). Remarkably, only 54 novel

lncRNAs were neither up- nor down-regulated in any of the conditions (>2-fold change, p <0.05).

Moreover, based on recent NET-seq data (Shetty et al. 2017), we estimated that about 87% of the

novel lncRNA genes are actively transcribed in proliferating or Spt5-depleted cells (Materials and

methods). Such active transcription included genes for which we could not detect the corresponding

lncRNAs by RNA-seq under the standard condition. These results argue against sequencing artefacts

and support that the turnover of these transcripts is modulated in response to different biological

conditions. Together, their low expression levels and induction under specialized conditions can

explain why the novel lncRNAs have not been identified in previous studies (Wilhelm et al. 2008;

Rhind et al. 2011; Eser et al. 2016).

In conclusion, these findings indicate that the novel lncRNAs comprise many cryptic transcripts

that are degraded by three main RNA-processing pathways during mitotic proliferation: the nuclear

exosome, the RNAi machinery, and the cytoplasmic exonuclease Exo2. The other RNA processing

factors analysed here seem to play only minor or redundant roles in lncRNA regulation. Many

lncRNAs become induced under specific physiological conditions when they might play specialized

roles.

Classification of lncRNAs into CUTs, DUTs and XUTs

In budding yeast, different groups of lncRNAs have been named according to the RNA-processing

pathways controlling their expression. For example, CUTs are targeted for degradation by the nuclear

exosome (Neil et al. 2009; Xu et al. 2009), and XUTs are targeted by the cytoplasmic exonuclease

Xrn1 (ortholog of *S. pombe* Exo2) (van Dijk et al. 2011). We introduce an analogous classification of

lncRNAs to provide a framework for analysis. Based on the panel of RNA-processing mutants tested here, the nuclear exosome, the cytoplasmic exonuclease, and the RNAi machinery are the three main pathways targeting lncRNAs (Figure 1 and Figure 3). These three pathways thus provide a natural way to classify the lncRNAs as CUTs and XUTs (corresponding to the budding yeast classes of the same names) and DUTs (Dicer-sensitive unstable transcripts). DUTs define a novel class not applicable to budding yeast which lacks the RNAi machinery.

Using a fuzzy clustering approach (Materials and methods), we classified both the novel and previously annotated lncRNAs that were significantly derepressed in at least one of the following mutants: *rrp6Δ* (CUTs), *dcr1Δ* (DUTs) or *exo2Δ* (XUTs). Of 7308 lncRNAs, 2068 remained unclassified because they were not significantly derepressed in any of the three mutants (1896 lncRNAs) or could not be assigned to a single class (172 lncRNAs). The remaining lncRNAs were classified into 2732 CUTs (493 annotated, 2239 novel), 1116 XUTs (181 annotated, 935 novel), and 1392 DUTs (209 annotated, 1183 novel). The resulting three classes were quite distinct (Figure 4A). These class associations are provided in Supplemental Tables S3 and S5. As expected, the lncRNAs of a given class were most highly expressed on average in the mutant used to define the class, although they were also more highly expressed in the other two mutants than in wild-type cells (Figure 4B). This pattern was also evident when clustering the three lncRNA classes separately based on the expression changes in the different RNA-processing mutants: lncRNAs of a given class were most highly derepressed in the mutant used to define this class, and in mutants affecting the same pathway, but they also tended to be derepressed in mutants of other pathways (Figure 4C). These results show that the lncRNAs of a given class are not exclusively derepressed in the mutant used to define this class. Thus, lncRNAs can be degraded by different pathways, although one pathway is typically dominant for a given lncRNA which is used here for classification.

Relationships between RNA-processing pathways targeting lncRNAs

To further dissect the functional relationships among the nuclear exosome, RNAi, and cytoplasmic exonuclease pathways, we attempted to construct double and triple mutants of *rrp6Δ, dcr1Δ* and *exo2Δ*. We could not obtain an *rrp6Δ exo2Δ* mutant from 24 tetrads dissected from the corresponding

cross. Among the tetrads analysed with three viable spores, the non-surviving spore was always of the *rrp6Δ exo2Δ* genotype, with a significant difference between observed and expected frequencies of wild-type, single and double mutant spores (chi-square test, p ~10^{-4}; based on 61% surviving spores). We conclude that the *rrp6Δ exo2Δ* double mutant is not viable. This synthetic lethality indicates that the nuclear exosome and cytoplasmic exonuclease together exert an essential role.

Conversely, the *exo2Δ dcr1Δ* and *rrp6Δ dcr1Δ* double mutants were viable, although the latter showed stronger growth defects than either single mutant (Supplemental Figure S3). While the *exo2Δ dcr1Δ* cells were elongated like the *exo2Δ* cells (Szankasi and Smith 1996), the *rrp6Δ* and *rrp6Δ dcr1Δ* cells were of normal length, with the double mutant looking more irregular and sick (Supplemental Figure S3). These findings suggest that the nuclear exosome and RNAi machineries can back each other up to some extent. We also attempted to construct an *rrp6Δ exo2Δ dcr1Δ* triple mutant by mating of the *exo2Δ dcr1Δ* and *rrp6Δ dcr1Δ* double mutants. This mating only produced ~17% viable spores, suggesting that the RNAi machinery is required for spore survival. As expected, we did not obtain any triple mutant among 24 tetrads dissected from this cross (chi-square test, p ~10^{-4}; based on 17% surviving spores). Thus, both the *rrp6Δ exo2Δ* double mutant and the *rrp6Δ exo2Δ dcr1Δ* triple mutant are not viable. Consistent with lncRNAs being targeted by multiple pathways (Figure 4B,C), these results point to some redundancy in function between the different RNA degradation pathways (Discussion).

We analysed the transcriptomes of the *exo2Δ dcr1Δ* and *rrp6Δ dcr1Δ* double mutants by RNA-seq. The *rrp6Δ dcr1Δ* double mutant showed a greater number of derepressed lncRNAs than either single mutant, especially among the novel lncRNAs (Figure 2; Figure 4C). The 5647 lncRNAs that were significantly derepressed in the *rrp6Δ dcr1Δ* double mutant (expression ratio >2, p <0.05) included 2653 CUTs and 1317 DUTs, but also 884 XUTs and 793 unclassified lncRNAs. This result again shows that the nuclear exosome and RNAi have partially redundant roles and can back each other up with respect to many RNA targets. Moreover, these two nuclear pathways can also degrade most XUTs that are further targeted by the cytoplasmic exonuclease. These findings highlight a prominent role of the joint activity of the nuclear exosome and RNAi to suppress a large number of lncRNAs.

In contrast, the *exo2Δ dcr1Δ* double mutant showed fewer derepressed XUTs and DUTs than either single mutant (Figure 2, Figure 4C). The 2272 lncRNAs that were significantly derepressed in the double mutant included only 675 XUTs and 658 DUTs, but 786 CUTs and 153 unclassified lncRNAs. This genetic suppression is consistent with the slightly diminished growth defect of the *exo2Δ dcr1Δ* double mutant compared to the *exo2Δ* single mutant (Supplemental Figure S3). Taken together, the complex findings from single and double mutants indicate that the three RNA-processing pathways can all target a wide range of lncRNAs, with differential preference for some targets, and channelling of lncRNAs to alternative pathways in the mutants. The higher numbers of derepressed lncRNAs in *rrp6Δ* and *dcr1Δ* mutants (Figure 2 and Figure 4C) indicate that most lncRNAs are degraded in the nucleus, most notably by the nuclear exosome.

Classification of lncRNAs by neighbouring mRNA positions

We also classified all known and novel lncRNAs into the main types based on their positions relative to the neighbouring mRNAs: Bidirectional, Antisense and Intergenic (Figure 5A). The criteria for these assignments, and overlaps between different classes, are specified in Materials and methods. In total, we defined 1577 Bidirectional (539 annotated, 1038 novel), 4474 Antisense (575 annotated, 3899 novel) and 1189 Intergenic (356 annotated, 833 novel) lncRNAs, besides 108 that overlapped mRNAs in sense direction (103 annotated, 5 novel; reflecting recent changes in TSS and TTS annotations in PomBase). Data for these lncRNA classes are provided in Supplemental Table S5. The Bidirectional lncRNAs were enriched for CUTs (Figure 5A). The Antisense lncRNAs were enriched for XUTs and, most notably, for DUTs, while the Intergenic lncRNAs were enriched for other, not classified lncRNAs (Figure 5A). Similar trends were also evident when analysing the lncRNA types the other ways round (Figure 5B): while most CUTs, DUTs and XUTs were Antisense, only the DUTs and XUTs were enriched for Antisense lncRNAs, while the CUTs were enriched for Bidirectional lncRNAs.

Expression patterns of lncRNAs

The expression of lncRNAs could be affected by the expression of neighbouring mRNAs, or it could actively control the expression of neighbouring mRNAs. To analyse the relationship between Bidirectional and Antisense lncRNAs and their associated mRNAs, we calculated the correlation coefficients for expression levels of each lncRNA-mRNA pair across all genetic and physiological conditions. Figure 5C shows that the expression of the Bidirectional lncRNAs tended to positively correlate with the expression of their associated mRNAs, for both the genetic and physiological conditions. The Antisense lncRNAs, on the other hand, revealed substantial differences for genetic vs physiological conditions. They mainly correlated negatively with sense mRNA expression in the physiological, but not in genetic conditions (Figure 5C). Thus, accumulation of Antisense lncRNAs in the different RNA-processing mutants is generally not sufficient to repress mRNA levels. These striking contrasts between the two lncRNA classes and different types of conditions provide clues about the lncRNA-mRNA expression relationships for Bidirectional and Antisense lncRNAs (Discussion).

The up-regulation of lncRNAs under specific physiological conditions (Figure 1 and Figure 3A) could reflect specialized roles under these conditions. We checked whether the different lncRNAs showed distinct regulatory patterns by clustering the classes separately based on their expression changes in the different physiological conditions. When clustering CUTs, DUTs and XUTs, the physiological conditions always clustered into three main groups that showed distinct patterns of lncRNA expression (Supplemental Figure S4): late meiosis, stationary phase (triggered by glucose limitation), and quiescence/early meiosis (both triggered by nitrogen limitation). These three groups reflect the major physiological states interrogated by the different conditions. The expression changes of CUTs, DUTs and XUTs, however, did not substantially differ across the physiological conditions. Most lncRNAs in all three classes, and among novel lncRNAs in particular, were strongly induced in late meiosis (Mei 8h; Figure 2, Supplemental Figure S4). Many lncRNAs were also induced during stationary phase and quiescence/early meiosis, with CUTs being relatively most conspicuous in these conditions (Figure 2 and Supplemental Figure S4).

We also analysed the lncRNAs classified by their positions relative to neighbouring mRNAs. As expected from Figure 5A,B, the nuclear exosome mutants showed the highest proportion of

derepressed Bidirectional lncRNAs but were also prominent in derepressing Antisense and Intergenic lncRNAs (Figure 6A). The *rrp6Δ dcr1Δ* double mutant led to derepression of a large number of lncRNAs, particularly Intergenic and Antisense lncRNAs (Figure 6A). Among the physiological conditions, late meiosis (Mei 8h) showed the highest proportions of induced lncRNAs for all three classes; this response was most notable for Antisense lncRNAs, many of which were highly induced, while much fewer Intergenic lncRNAs were induced (Figure 6A and B). Overall, the Bidirectional, Antisense and Intergenic lncRNAs showed stronger class-specific expression signatures in the physiological conditions than did the CUTs, XUTs and DUTs (Figure 6B *vs* Supplemental Figure S4). But expression patterns across the different physiological conditions were not sufficiently distinct to predict class membership based on these patterns.

Nucleosome profiles of lncRNA regions

Transcribed regions are often accompanied by distinct patterns of nucleosome distribution. As a proxy for nucleosome distributions around lncRNA regions, we sequenced mononucleosomal DNA to compare the chromatin organization between protein-coding and non-coding transcribed regions in proliferating wild-type cells. We only analysed lncRNA regions that did not overlap with any mRNA regions to minimize confounding data from coding transcription (although some mRNA transcription start sites may remain among the Bidirectional lncRNA data). Figure 7 shows that both Bidirectional and Intergenic lncRNAs initiated in nucleosome-depleted regions, at the 5'-end of a positioned nucleosome. This feature was shared with mRNA regions, although these regions showed much higher nucleosome densities and a higher order of subsequent nucleosomes. In general, intergenic regions showed lower nucleosome densities than did mRNA regions, as has been observed before (Lantermann et al. 2010). We conclude that there are both similarities (around the transcription start site) and differences in chromatin organization between coding and non-coding regions.

Translation of lncRNAs

Ribosome profiling before and during meiotic differentiation has revealed that as much as 24% of the annotated lncRNAs are actively translated (Duncan and Mata 2014). Such translation typically

increases during meiosis and involves short open reading frames (ORFs), often more than one per lncRNA. In addition, translation has been detected in numerous unannotated regions of the genome (Duncan and Mata 2014). We analysed the ribosome-profiling data from Duncan and Mata (2014), covering the whole genome of proliferating and meiotic cells, to assess translation of the different classes of annotated and novel lncRNAs defined above. Details of all 771 translated non-coding regions are provided in Supplemental Table S6.

Table 1 shows the numbers and percentages of actively translated lncRNAs, both for all translated regions of at least one codon and for a conservative set of translated regions with at least ten codons. Overall, the novel lncRNAs showed a much lower proportion of translated transcripts than the annotated lncRNAs. This result likely reflects their lower expression levels (Figure 3B). Such low expression makes it harder to obtain sufficient ribosome-profiling reads to determine translation for most lncRNAs, especially because no ribosome profiling data were available for most conditions in which the novel lncRNAs became derepressed. Nevertheless, 66 or 148 novel lncRNAs were found to be actively translated using the more or less conservative cutoff, respectively. Among the main classes, the Bidirectional lncRNAs showed the largest numbers and proportions of translated RNAs, which were highly enriched (Table 1; $p = 1.7e^{-26}$). Moreover, up to 30% of the 108 previously annotated lncRNAs overlapping mRNAs in sense direction were actively translated. This finding suggests that some of these RNAs are alternative 'untranslated regions' of the mRNAs with translation of short upstream ORFs (Duncan and Mata 2014).

It is not clear to what extent any stable, functional peptides are generated by all this translational activity. The engagement of lncRNAs with ribosomes could trigger NMD and degradation via the cytoplasmic exonuclease (de Andres-Pablo et al. 2017; Quinn and Chang 2016; Malabat et al. 2015). We therefore checked whether the translated lncRNAs were enriched among those being derepressed in the *upf1Δ* mutant which is defective for NMD (Rodríguez-Gabriel et al. 2006). There were no significant overlaps between the translated RNAs and the novel, annotated or all lncRNAs derepressed in *upf1Δ* cells. Moreover, despite including several translated lncRNAs, the Bidirectional lncRNAs showed no significant overlap with RNAs derepressed in *upf1Δ* cells. This finding is consistent with Bidirectional lncRNAs being mainly targeted by the nuclear exosome rather

than the cytoplasmic exonuclease (Figure 5A and B). Conversely, the translated XUTs and Antisense lncRNAs were both significantly enriched for RNAs derepressed in *upf1Δ* cells (p = $6.7e^{-24}$ and $1.5e^{-25}$, respectively). This result is consistent with the cytoplasmic exonuclease being the major pathway for NMD-mediated RNA degradation. Together, these findings suggest that engaging with ribosomes triggers the degradation of some XUTs and Antisense lncRNAs, but not of Bidirectional lncRNAs which are thus more likely to produce peptides.

DISCUSSION

This study has uncovered 5775 novel lncRNAs, 1026 of which are high confidence based on sequence-read coverage. Our annotation is optimized for sensitivity at the cost of specificity. From our web viewer (http://bahlerlab.info/ncViewer), it is clear that some lncRNAs might consist of transcribed regions encompassing several smaller RNAs or variable, condition-specific isoforms. Annotations of lncRNAs are currently approximate in essentially all systems analysed, and RNA-seq data have clear limitations for mapping of TSS and TTS. Nevertheless, the broad, approximate annotations of lncRNAs (or transcribed regions) under diverse conditions are a useful framework for future research on lncRNA function.

Compared to mRNAs and previously annotated lncRNAs, the novel lncRNAs are subject to stronger and more widespread differential expression, mostly induction, in response to multiple genetic and physiological conditions. Analysis of lncRNA expression across a broad panel of RNA-processing mutants indicates that the nuclear exosome, the RNAi pathway and the cytoplasmic exonuclease are key pathways targeting lncRNAs. Analogous to budding yeast, we have classified lncRNAs into CUTs, DUTs and XUTs, defined by the pathway which preferentially degrades them. Notably, mRNAs are much less affected by the absence of these RNA-processing pathways than are lncRNAs (Figures 1-3), suggesting that lncRNAs are important targets of these pathways. Unstable lncRNAs have been most extensively described at a genome-wide level in budding yeast which

guided our classification. The lncRNA classes defined here show both similarities and differences to the classes defined in budding yeast, as highlighted below.

The ~2000 budding yeast CUTs are derepressed upon deletion of the nuclear-specific exosome subunit Rrp6 and transcribed divergently from mRNAs with which they positively correlate in expression (Neil et al. 2009; Xu et al. 2009). These findings are similar to our results (Figure 4 and Figure 5). A difference, however, is that budding yeast CUTs are greatly stabilized by loss of Trf4, a key component of the exosome-targeting TRAMP complex (Wlotzka et al. 2011; Frenk et al. 2014), while fission yeast CUTs are only marginally affected by loss of the TRAMP subunit Cid14 (Figure 1 and Figure 2), as shown before (Zhou et al. 2015). This result indicates a TRAMP-independent mechanism of exosomal degradation of CUTs in fission yeast. Indeed, the polyA-binding protein Pab2, functioning in a complex called MTREC, targets meiotic or unspliced mRNAs and lncRNAs in fission yeast (Yamanaka et al. 2010; McPheeters et al. 2009; Lee et al. 2013; Egan et al. 2014; Zhou et al. 2015; St-André et al. 2010). Our data support a Pab2-dependent mechanism for targeting CUTs, showing a stronger derepression of CUTs in *pab2* mutants than in *cid14* mutants, although both mutants show much smaller effects than the exosome mutants *rrp6* and dis3 (Figures 1-3). Also in human cells, many lncRNAs are targeted for exosomal degradation by PABPN1, an ortholog of Pab2 (Beaulieu et al. 2012; Meola et al. 2016). Reminiscent of yeast CUTs, exosome depletion in mammals has revealed lncRNAs divergently transcribed from promoter regions of protein-coding genes (Quinn and Chang 2016; Grzechnik et al. 2014; Jensen et al. 2013). Whether the evolutionary conservation of this principle reflects functional importance of CUTs or their transcription, or simply that they are non-functional by-products of the basic mechanics of transcription, remains an open question.

The ~850 SUTs in budding yeast are detectable in proliferating wild-type cells, and are processed differently from CUTs (Neil et al. 2009; Tuck and Tollervey 2013). SUTs could be considered analogous to the previously annotated lncRNAs in fission yeast, which can be readily detected in proliferating wild-type cells (Wilhelm et al. 2008; Rhind et al. 2011) and show less variable expression than novel lncRNAs across the different conditions (Figure 3A). CUTs and SUTs almost exclusively originate from nucleosome-depleted regions at the ends of coding genes (Jensen et

al. 2013). Our nucleosome-profiling data also suggest a strong tendency of Bidirectional and

Intergenic lncRNAs to initiate in nucleosome-depleted regions upstream of positioned nucleosomes

(Figure 7). These nucleosome data are only approximate, as we did not determine the profiles under

the different genetic or physiological conditions when lncRNAs are more highly expressed.

The ~1700 budding yeast XUTs are derepressed upon deletion of the cytoplasmic exonuclease

Xrn1 (ortholog of *S. pombe* Exo2), and are mostly antisense to mRNAs and anti-correlate with sense

expression (van Dijk et al. 2011). These findings resemble our results (Figure 4 and Figure 5), and

related recent findings in *S. pombe* (Wery et al. 2018). The targeting of XUTs by a cytoplasmic

exonuclease implies their efficient export to the cytoplasm. However, the proposed inhibitory

functions of XUTs on coding transcription are likely mediated co-transcriptionally, and so the

relevance of their cytoplasmic export is unclear (Hansen et al. 2013; Tuck and Tollervey 2013). In

budding yeast, XUTs are targeted by the NMD pathway before being degraded by Xrn1, and this

pathway can be regarded as the last filter to dampen lncRNA expression (Malabat et al. 2015; Wery et

al. 2016). Consistent with the cytoplasmic exonuclease acting as a backup system, we find that many

CUTs and DUTs are also targeted by Exo2 and the NMD factor Upf1 (Figure 2 and Figure 4C). Our

XUTs and Antisense lncRNAs that engage with ribosomes, but not other classes of lncRNAs, are

significantly enriched for RNAs derepressed in *upf1Δ* cells, supporting a role of the NMD in Exo2

degradation. Although there are overlaps of lncRNA expression in the absence of Upf1 and Exo2,

much fewer lncRNAs are derepressed in *upf1* than in *exo2* mutants (Figure 2 and Figure 4C).

Absence of two other regulators of cytoplasmic RNA degradation, Ski7 and Pan2 (Lemay et al. 2010;

Wolf and Passmore 2014), has only subtle effects on lncRNA derepression (Figure 2 and Figure 4C).

These results suggest that Exo2 plays the major role and can degrade lncRNAs independently of these

other factors. However, a limitation of the current study is that RNA-seq only measures steady-state

RNA levels, which integrates transcription and degradation. Findings from budding yeast indicate

that mRNA levels can be adjusted by buffering mechanisms, allowing compensation of increased

degradation by increased transcription or *vice versa* (Haimovich et al. 2013; Sun et al. 2017). Xrn1,

the Exo2 ortholog, is required for this buffering. So it is possible that the weak derepression

phenotypes of cytoplasmic RNA degradation mutants, other than exo2, reflect that lncRNA levels are

efficiently buffered in these mutants. More work is required to investigate whether the buffering system is conserved in fission yeast and whether lncRNAs are subject to it.

Budding yeast has no analogous lncRNA class to the DUTs defined here, because the RNAi pathway is missing (Harrison et al. 2009). Our results show that RNAi is important to control lncRNA expression in fission yeast, most notably Antisense lncRNAs that are derepressed in late meiosis (Figure 5 and Figure 6). In fission yeast, RNAi can dampen RNA expression via either transcriptional or post-transcriptional mechanisms (Castel and Martienssen 2013; Smialowska et al. 2014). Our data do not allow to distinguish between these two possibilities. Although RNAi is not required for antisense-mediated transcriptional repression at three meiotic mRNAs (Chen et al. 2012), our and other results (Bitton et al. 2011) indicate a prominent global role of RNAi to suppress many Antisense lncRNAs. About 75% of all DUTs are Antisense lncRNAs. RNAi plays an even more important role than Exo2 in repressing Antisense lncRNAs, but also targets Bidirectional and Intergenic lncRNAs (Figure 5A and B). It is not clear whether the RNAi machinery is involved to a similar extent in controlling lncRNAs in multicellular organisms.

NUTs are another class of unstable lncRNAs in budding yeast, which substantially overlap with CUTs and XUTs (Schulz et al. 2013). NUTs are detected upon depletion of Nrd1, a member of the Nrd1-Nab3-Sen1 (NNS) complex that promotes transcriptional termination of lncRNAs (Schulz et al. 2013). NNS also plays an important role in recruiting TRAMP for degradation of its targets (Tudek et al. 2014). No NNS complex was identified in fission yeast, and depletion of Seb1 impairs polyA-site selection but not RNA abundance (Lemay et al. 2016; Wittmann et al. 2017). Thus, a class corresponding to NUTs does not appear to exist in fission yeast. This conclusion is also consistent with Pab2, rather than TRAMP, being more important for exosome-mediated degradation of lncRNAs.

The different lncRNA classes based on RNA-processing pathways, while useful, are fairly arbitrary and overlapping. The lncRNAs are targeted by multiple redundant or coordinating pathways in an intricate backup system, although one pathway is often dominant for a given lncRNA. This property has also been documented in budding yeast (Marquardt et al. 2011). Moreover, RNA-processing mutants can lead to cellular re-routing of RNA degradation. Accordingly, there are

substantial overlaps between different lncRNA classes in both budding and fission yeast. We find

that cells require either the nuclear exosome or cytoplasmic exonuclease to survive, with the absence

of both pathways being lethal. While these pathways function in other aspects of RNA metabolism,

this synthetic lethality points to the importance of dampening the extensive lncRNA expression,

which are much more affected in the corresponding mutants than are mRNAs (Figure 2). It is

possible that the cytoplasmic exonuclease can serve as a backup to degrade transcripts that escaped

degradation by the nuclear exosome. On the other hand, cells survive without the cytoplasmic

exonuclease and RNAi or without the nuclear exosome and RNAi. Surprisingly, cells lacking both

the cytoplasmic exonuclease and RNAi show fewer derepressed XUTs and DUTs than cells lacking

only one of these pathways (Figure 2). This suppression might reflect that lncRNAs that cannot be

degraded by RNAi are effectively targeted by the nuclear exosome. Consistent with this possibility,

absence of both the nuclear exosome and RNAi leads to poor growth and large numbers of

derepressed lncRNAs (Figure 2, Supplemental Figure S3). These findings indicate partially

redundant roles for the nuclear exosome and RNAi pathways, which can back each other up with

respect to many RNA targets. These two nuclear pathways can also degrade most XUTs that are

further targeted by the cytoplasmic exonuclease. The RNAi and exosome pathways in fission yeast

have overlapping functions to repress aberrant transcripts (Buhler et al. 2008; Zhang et al. 2011;

Zofall et al. 2009) as well as meiotic mRNAs and other genomic regions (Yamanaka et al. 2013,

2010; Sugiyama and Sugioka‑Sugiyama 2011). Our study highlights that the nuclear exosome and

RNAi pathways also cooperate to suppress thousands of lncRNAs.

The expression levels of most lncRNAs are highly induced in non-dividing states (stationary

phase and quiescence) and during meiotic differentiation, most notably in late meiosis when over

3000 Antisense lncRNAs are induced (Figure 1 and Figure 6). These results raise the possibility that

lncRNAs function during these conditions. It is known that unstable lncRNAs, normally targeted for

rapid degradation, can become stabilised and functional under specialized conditions (Camblong et al.

2007; Houseley et al. 2008). Environmentally regulated changes to RNA quality-control activities

can alter transcriptomes and mediate stress responses (Joh et al. 2016). RNA-processing pathways

might become down-regulated under certain physiological conditions, allowing lncRNAs to accumulate. The mRNA levels of relevant RNA-processing genes do not strongly change in response to our physiological conditions, although mRNAs encoding nuclear-exosome components decrease ~2.7-fold during meiosis (Bitton et al. 2015a). Many meiotic mRNAs are repressed in mitotic cells by the RNAi and exosome pathways and derepressed during meiosis (Yamanaka et al. 2013, 2010; Sugiyama and Sugioka‑Sugiyama 2011). Derepression of lncRNAs during meiosis and other specialized conditions could involve similar regulation. Indeed, our findings indicate that Exo2 also plays an important role in repressing many lncRNAs, but also many middle meiotic genes (Mata et al. 2002) that are derepressed in *exo2* mutants and meiosis. These results put Exo2 on the map as an important new regulator of meiotic gene expression.

In addition to derepression, the induction of lncRNAs could involve increased transcription (Castelnuovo et al. 2014). RNA-processing factors likely regulate RNA levels via coordinated interplays between transcription and degradation (Haimovich et al. 2013; Sun et al. 2017), and changes in this coordination could lead to the accumulation of different lncRNAs in different physiological conditions. Our data cannot distinguish between lncRNA regulation at the level of transcription or RNA decay.

Antisense transcripts are the most widespread class of lncRNAs. It has recently been reported that differences in polyA sites between convergent genes generate distinct antisense landscapes in budding and fission yeast (Liu et al. 2017). In our data, over 70% of coding sequences produce at least one Antisense lncRNA from the other strand. This finding complements and extends previous analyses on antisense transcription in fission yeast (Wilhelm et al. 2008; Dutrow et al. 2008; Ni et al. 2010; Rhind et al. 2011; DeGennaro et al. 2013; Eser et al. 2016; Chen et al. 2012; Bitton et al. 2011; Zofall et al. 2009; Clément-Ziza et al. 2014; Zhang et al. 2011; Marguerat et al. 2012; Wery et al. 2018). Antisense lncRNAs include CUTs, DUTs, XUTs and other lncRNAs, with XUTs and especially DUTs being strongly enriched (Figure 5A,B). Thus, several RNA processing pathways can be involved in controlling Antisense lncRNAs. Previous studies have reported repressive effects of Antisense lncRNAs on their sense mRNAs (Bitton et al. 2011; Chen et al. 2012; Leong et al. 2014; Ni

et al. 2010; Marguerat et al. 2012; Wery et al. 2018). Accordingly, we find a strong global tendency towards anti-correlation between Antisense lncRNA-mRNA expression levels under physiological conditions (Figure 5C). In contrast, Antisense lncRNA expression shows a slight tendency towards positive correlation with mRNA expression under the genetic conditions (Figure 5C). Thus, stabilization of Antisense lncRNAs in the absence of different RNA-processing factors appears generally not to be sufficient for mRNA repression. This finding suggests that Antisense lncRNAs often control mRNA expression at the level of transcription (*e.g.* by transcriptional interference or altered chromatin patterns) rather than functioning as transcripts. Alternatively, many Antisense lncRNAs might simply reflect opportunistic transcription, enabled by down-regulation of the dominant, overlapping mRNAs, with the anti-correlated expression reflecting passive, indirect effects. The ~29% of protein-coding regions not associated with Antisense lncRNAs are enriched for highly expressed genes, suggesting that these genes are either protected from, or interfere with, antisense transcription. Despite the global anti-correlation (Figure 5C), large numbers of Antisense lncRNAs go against this trend, indicating that the expression relationships between lncRNAs and mRNAs involve multiple processes and cannot be explained by a few regulatory or indirect mechanisms. This conclusion is consistent with the diverse findings on antisense lncRNA processes in other organisms (Pelechano and Steinmetz 2013; Mellor et al. 2016).

Conclusions

This study increases the number of lncRNAs annotated in fission yeast by almost 5-fold, revealing both similarities and striking differences to lncRNA characteristics and regulation budding yeast. The novel lncRNAs are typically very lowly expressed but become derepressed in response to different genetic and physiological perturbations. In stark contrast, the mRNAs and annotated lncRNAs show less widespread changes in expression, especially in the genetic perturbations. The nuclear exosome, RNAi machinery, and cytoplasmic exonuclease are the dominant RNA-processing pathways degrading lncRNAs, used to define the CUTs, DUTs and XUTs, respectively. Bidirectional lncRNAs are enriched for CUTs and translating ribosomes, and positively correlate with divergent mRNA

expression. Antisense lncRNAs are enriched for DUTs and XUTs, are mostly derepressed in late

meiosis, and negatively correlate with sense mRNA expression in physiological, but not in genetic

conditions. Intergenic lncRNAs are enriched for lncRNAs that are not classified as CUTs, DUTs or

XUTs. The transcripton of Intergenic and Bidirectional lncRNAs initiates from regions that in wild-

type cells are nucleosome-depleted, just upstream of a positioned nucleosome. Given their low

expression and other features, it seems likely that any regulatory functions mediated by most

lncRNAs are in *cis* and co-transcriptional.

Our findings highlight a substantial role of RNAi, in coordination with the nuclear exosome, in

controlling a large number of lncRNAs typified by the new class of DUTs. Moreover, the findings

reveal a prominent new function of the Exo2 cytoplasmic exonuclease, together with RNAi, in

dampening the expression of both lncRNAs and mRNAs that become derepressed during meiosis.

The nuclear exosome and cytoplasmic exonuclease together play an essential role for cell viability.

The three RNA-processing pathways show overlapping roles and can target most lncRNAs with

different affinities, forming an intricate, intertwined RNA-surveillance network. Besides these

biological insights, this study provides broad data on diverse lncRNA characteristics and a rich

resource for future studies on lncRNA functions in fission yeast and other organisms.

MATERIALS AND METHODS

S. pombe strains

All strains, physiological and growth conditions (Edinburgh minimal media, EMM2, or Yeast Extract

media, YE), and biological repeats used for RNA-seq in the current study are detailed in

Supplemental Tables S1 and S2. Biological repeats are based on independent cell cultures of the

different strains. The number of different samples was decided to broadly interrogate key genetic and

physiological conditions, balancing biological insight with costs. The PCR-based approach (Bähler et

al. 1998) was used for gene deletions of *exo2, pan2*, and strains used to generate double mutants.

Double mutants among *dcr1*, *rrp6* and *exo2* were created by crossing the corresponding single

mutants (Supplemental Table S1). Strain *h⁻ dcr1::nat ura4⁻* was generated using the PCR-based approach (Bähler et al. 1998). Random spore analysis was used to create the other single mutant strains with the correct mating-types. Strains were crossed and incubated on malt extract agar (MEA) for 2-3 days at 25°C. Tetrads were treated with zymolyase (0.5 mg/ml, MP Biomedicals Europe) and incubated at 37°C for at least 4 h to release spores. Spores were germinated on YE agar plates before being replica plated to selective EMM2 plates as appropriate. All deletion junctions were PCR verified (Bähler et al. 1998). Crosses and selection by random spore analysis were as follows: *h⁺ ade6-M216 leu1-32 ura4-D18 his3-D1 rrp6::ura4* was crossed with *h⁻ ura4-D18* with selection on EMM2 plates to create *h⁺ rrp6::ura4 ura4-D18; h⁻ exo2::kanMX6 ade6-216* was crossed with *h⁺ ura4-D18* with selection on YE + kanamycin plates, and on EMM2 plates with or without uracil, to select for *h⁺ exo2:: kanMX6 ura-D18* and *h⁻ exo2:: kanMX6 ura-D18*. Tetrad analysis was used to analyse the meiotic products resulting from the crosses in all combinations of the *rrp6Δ, dcr1Δ* and *exo2Δ* single mutant strains. Strains were crossed and incubated on MEA plates for 2-3 days at 25°C. The resulting tetrads were dissected using a micromanipulator (Singer Instruments), and spores germinated on YE plates after 5 days of growth. Haploid colonies arising from germinated spores were then streaked to selective plates to test for KAN, NAT and URA markers. All deletion junctions in double-resistant colonies were PCR-verified (Bähler et al. 1998).

Growth conditions

All mutant cell cultures were harvested at mid-log phase (optical density, $OD_{595} = 0.5$). For stationary-phase experiments, wild-type cells were grown in EMM2 at 32°C. A sample representing 100% survival was harvested when cultures reached a stable maximal density. Colony forming units (CFUs) were measured every 24 hours after this initial time-point, and another sample harvested when cultures reached 50% survival. For quiescence experiments, cells were grown in EMM2 at 32°C an OD_{600} of 0.2, before being centrifuged, washed twice in EMM2 without nitrogen (NH_4Cl) and cultured in EMM2 without nitrogen at 32°C. Cells under nitrogen starvation reached an OD_{600} of 0.8 within 24 hours, and were harvested at 24 hours and 7 days after nitrogen removal. For meiotic timecourses, *pat1-114* diploid cells were grown to mid-log phase before being shifted to EMM2

without nitrogen. Cells were incubated at 25°C overnight to synchronise them in G1 phase. Meiosis was induced by addition of NH_4Cl to final concentration of 0.5 g/L and incubation at 34°C (0 hour timepoint). Cells were harvested by centrifugation of 50 ml cultures at 2300 rpm for 3 min, and pellets were snap-frozen and stored at -80°C prior to RNA extraction.

RNA-seq experiments and initial analyses

RNA was extracted from harvested cells using a hot-phenol method (Bähler and Wise 2017). The quality of total extracted RNA was assessed on a Bioanalyser instrument (Agilent). Strand-specific RNA-seq libraries were prepared using an early version of the Illumina TruSeq Small RNA Sample Prep Kit. For polyA-enriched samples, library preparation and sequencing protocols were as described (Lemieux et al. 2011), and for samples depleted for rRNAs (*rrp6Δ, exo2Δ*), as described (Bitton et al. 2014). RNA-seq libraries were sequenced on an Illumina HiSeq 2000 instrument, using single-end runs with 50 bp reads (The Berlin Institute for Medical Systems Biology, Germany). Reads were aligned to the fission yeast genome with the exonerate software (Slater and Birney 2005). The few reads which mapped equally well to multiple genomic locations were assigned at random to one of these locations. Reads containing up to 5 mismatches (not clustered at read ends) were kept for further analysis. For a previous study (Marguerat et al. 2012), we performed mapping quality tests to show that 5 mismatches work well for the *S. pombe* genome which has few repetitive regions. Between 20 and 50 million mappable reads were obtained for each library (~80-85% of total reads were mappable). Expression scores were calculated for annotated features using the genome annotation available in PomBase on 9th May 2011 (Wood et al. 2012), and *in house* Perl scripts as described (Marguerat et al. 2012). Reads per kilobase of transcript per million reads mapped (RPKMs) for annotated features correlated strongly between biological replicates ($r_{Pearson}$ >0.98). Mapping and expression score pipelines were performed essentially as described (Lemieux et al. 2011). The reads were mapped only to the genome, and the reads were aligned in Exonerate using the default (ungapped) mode.

Segmentation of sequence data to define novel lncRNAs

Custom scripts for segmentation of RNA-seq data were written in *R* and *Perl*. A simple heuristic was

designed to detect novel lncRNAs from RNA-seq data. This segmentation heuristic was optimised

for its ability to detect the 1557 annotated lncRNAs, and validated by visual inspection of RNA-seq

data. The following RNA-seq data from initial sequencing runs were pooled (2 biological repeats

each): *rrp6-ts, exo2Δ, dis3-54, pab2Δ, nmt1-mtr4* (Lemay et al. 2014; Bitton et al. 2015a)*, ago1Δ,*

rdp1Δ, dcr1Δ, pan2Δ, upf1Δ, Stat 100%*,* Stat 50%*,* Quies 24 h, Quies 7d, Meiotic pool (Schlackow et

al. 2013), YE1, and Reference (control) (Supplemental Tables S1 and S2). Segments were delimited

from the pooled data using a 10 hits/bp cut-off. This approach improves the signal-to-noise ratio to

increase sensitivity at the cost of specificity. However, nearly 100% of the novel lncRNAs were

retained also when using only single samples, without pooling, applying the same threshold of >10

reads/bp for at least 1 sample. Thus, the final count of lncRNAs was not inflated by pooling of

multiple conditions in which lncRNAs showed ≤10 reads. The advantage of having multiple diverse

conditions was to uncover lncRNAs expressed only under specific conditions, and were therefore

missed in previous analyses. Segments <100 bp apart and differing in pooled read density (average

hits/bp of segment) by <10-fold were joined together. The ability to detect the annotated 1557

lncRNAs was judged on the percentage coverage of each segment overlapping a lncRNA, and the

percentage coverage of each lncRNA overlapping a segment. To optimize these two values, we

varied the following parameters: 1) hits/bp cut-off, 2) fusing distance, 3) imposing rule on whether to

fuse based on fold difference in expression of consecutive segments, and 4) varying this fold

difference in expression at which consecutive segments were fused. Imposition of the criterion that

consecutive segments should only be fused if their fold difference in expression meets a certain

threshold aimed to detect lncRNAs near, but distinct from, mRNAs, while discarding data which

likely represent misannotated untranslated regions. With the optimized segmentation procedure,

annotated lncRNAs were covered at 92% by the detected segments.

Using the PomBase genome annotation (May 2011), segments overlapping annotations on the

same strand, including untranslated regions, were removed. We discarded segments of <200 bp as

lncRNAs are defined by an arbitrary minimal length cut-off of 200 nt (Mattick and Rinn 2015),

reflecting RNA-seq library protocols that exclude small RNAs. The remaining consecutive segments

>200 bp defined 5775 novel lncRNAs. Overall, 214 of the 487 novel lncRNAs reported by Eser et al.

(2016) could not be validated using our segmentation (Supplemental Table S4). This analysis revealed

that TSS uniquely called by Eser et al. (2016) show no signal in our RNA-seq data in any of the

conditions, yet they often correspond to very strong signal from the opposite strand. These patterns

raise the possibility that many of the 214 lncRNAs exclusively called by Eser et al. (2016) might be

artefacts based on 'leak-through' of the opposite-strand signal, which can result from some sequence

library protocols (Perocchi et al. 2007).

To further verify the robustness of our segmentation, we applied the RNA-seq segmentation

algorithm published by Eser et al. (2016) to annotate the TSS for all RNAs (coding and non-coding)

in each of three of our key datasets: *dcr1, exo2, rrp6* mutants. We used a detection threshold

calculated by a bimodal distribution model, min-length of 200 and max-gap equal 80. The detection

thresholds (reads per bp) with our *dcr1, exo2,* and *rrp6* mutant data were 11.1, 7.6, and 9.7,

respectively. We checked which of these TSS called by Eser's method overlap with previously

annotated or novel ncRNAs. This analysis revealed that 4252 of 9100 called TSS in *dcr1* mutants

overlap with 3332 RNAs (2587 annotated, 745 novel), 4991 of 9810 called TSS in *rrp6* mutants

overlap with 3939 RNAs (3004 annotated, 935 novel), and 4426 of 9377 called TSS in *exo2* mutants

overlap with 3519 RNAs (2671 annotated, 848 novel). The data for these overlaps are provided in the

last three columns of Supplemental Table S3. We then asked whether Eser's method detected much

fewer novel ncRNAs than mRNAs, which would signify differences in the annotation quality between

the two categories. However, Eser's method finds similar proportions of mRNAs and novel ncRNAs

in the three mutant datasets (*dcr1* mutant: 29.2% mRNAs, 22.6% ncRNAs; *exo2* mutant: 30.7%

mRNAs, 24.0% ncRNAs; *rrp6* mutant: 36.2% mRNAs, 25.4% ncRNAs). This analysis shows that the

novel ncRNAs are nearly as likely to be called by Eser's method as are the mRNAs, although the

latter are much more highly expressed. We therefore conclude that novel ncRNA annotations can be

detected almost as effectively by Eser's method as mRNAs.

We also compared the XUTs reported by Wery et al. (2018) to our annotations. Wery et al.

define 1628 XUTs mapping to Chromosomes I-III, of which 1228 overlap with 1150 lncRNAs (575

annotated, 575 novel), and of which we classified 299, 315 and 84 as XUTs, CUTs and DUTs,

respectively. These differences reflect the different samples used to define the XUTs. While the XUTs

annotated by Wery et al. (2018) are induced in the *exo2* mutant, many are even more induced in *rrp6*

or *dcr1* mutants, and we therefore defined them as CUTs or DUTs, respectively. The overlaps of the

XUTs defined by Wery et al. (2018) with annotated or novel lncRNAs are indicated in Supplemental

Table S3.

We defined three confidence classes based on RPKM values from all sequenced samples as

follows: high confidence lncRNAs had ≥10 RPKM in at least one sample; medium confidence

lncRNAs had <10 RPKM but ≥1 RPKM in at least one sample; and low confidence lncRNAs had <1

RPKM in all samples. We have set up a web tool to view the RNA-seq data for all lncRNAs and

mRNAs in the different conditions (http://bahlerlab.info/ncViewer).

Analyses of RNA expression

Novel lncRNAs defined by the segmentation process described above, together with all annotated

transcripts, were analysed using the Bioconductor DESeq2 package (Love et al. 2014). Differentially

expressed genes were defined as those being >2-fold induced (average of two biological repeats) or

repressed and showing significant changes (adjusted $p <0.05$) compared to three reference samples as

determined by DESeq2. For hierarchical clustering of expression data, log2 ratios were clustered in R

with the pheatmap package, using the Euclidian distance measure and the ward.D or ward.D2

clustering options. For expression correlation analyses, we evaluated the similarity of expression

levels of Bidirectional and Antisense lncRNAs to the expression levels of their neighbouring mRNAs

using normalised expression values across the entire dataset. Vectors of mRNA-lncRNA pairs were

generated and Pearson's correlation coefficients were computed. For lncRNAs associated with

multiple mRNAs, only the nearest mRNA was considered. Functional enrichments of gene lists were

performed using the AnGeLi tool which applies a 2-tailed Fisher's exact test (Bitton et al. 2015b).

To test for nascent transcription of lncRNA genes, we analysed recently published data from

native elongating transcript sequencing (NET-seq) (Shetty et al. 2017). Normalised NET-seq data of

proliferating cells (with or without depleted of Spt5) in 'WIG' format were downloaded from GEO (accession: GSM2258030). The NET-seq targets the 3'-end of nascent transcripts, and we systematically computed the normalised NET-seq signal across the entire lengths of the novel lncRNAs. The lncRNAs were considered present when signal was >0 in at least one replicate in any condition. The low threshold was required owing to the very low read numbers in the NET-seq data. This analysis suggested that 87.4% of all lncRNAs are transcribed in proliferating cells. Given the limited sensitivity of the NET-seq data, we expect this number to be a lower estimate.

Classification into CUTs, DUTs and XUTs

Differential expression data from *dcr1Δ*, *exo2Δ* or *rrp6Δ* mutants were filtered to retain only transcripts that were significantly induced in ≥1 mutant compared to wild-type controls (expression ratio >2 and adjusted p-value < 0.05). RPKM values from independent biological repeats for the differentially expressed RNAs were then standardized to have a mean value of 0 and a standard deviation of 1, followed by clustering using the Mfuzz clustering function in R (Kumar and E. Futschik 2007). The number of clusters "c" was set to 3 and the fuzzification parameter "m" to 1.25. To further reduce ambiguity when associating RNAs to clusters, the minimum membership value of a lncRNA belonging to a specific cluster was set to 0.7 (Kumar and E. Futschik 2007). For this classification, more recent PomBase annotations were used which contained only 1533 annotated lncRNAs (7308 annotated and novel lncRNAs in total).

Classification into Bidirectional, Antisense and Intergenic lncRNAs

To assess whether a given annotated or novel lncRNA overlaps with any mRNAs in either orientation, we systematically aligned the lncRNA coordinates relative to the annotation in Ensembl *S. pombe*, Assembly ASM294v2, release 33 (Flicek et al. 2014), enhanced by a modified annotation set that better delineates transcript boundaries. To this end, we exploited Transcription Start Sites (TSS) determined using Cap Analysis of Gene Expression (CAGE) (Li et al. 2015) and Transcription Termination Sites (TTS) defined using genome-wide polyadenylation site mapping (Mata 2013). For

genes without these higher quality boundaries, we used the annotated TSS and TTS. All TSS and

TTS used are provided in Supplemental Table S7. We called overlaps in either orientation when ≥1

nt was shared between transcripts. Using the same criteria, we tested for overlaps with novel

lncRNAs that have recently been reported (Eser et al. 2016) (Supplemental Table S4).

Using these overlap criteria, we classified all known and novel lncRNAs based on their

proximity to nearby mRNAs. We defined lncRNAs as Intergenic if they do not overlap with any

nearby mRNA, Sense-overlapping lncRNAs if they overlapped with any mRNA on the same strand,

Antisense if they overlap ≥1 nt with a mRNA on the opposite strand, and Bidirectional if their TSS

was <300 nt up- or down-stream of a TSS of a mRNA on the opposite strand. Naturally, given the

compact fission yeast genome, there was some overlap between these classes. We reassigned

lncRNAs present in two classes using the following criteria. The lncRNAs classified as both

Bidirectional and Intergenic (482 lncRNAs) or as Bidirectional and Antisense (1068 lncRNAs) were

assigned to Bidirectional lncRNAs only. The 135 lncRNAs classified as both Sense-overlapping and

either 86 Antisense or 49 Bidirectional lncRNAs were, respectively, assigned to Antisense or

Bidirectional lncRNAs only.

Translation analysis of lncRNAs

For the ribosome profiling analysis, we systematically looked for overlaps between the translated

regions defined before (Duncan and Mata 2014) and all annotated and novel lncRNAs. The

significance of enrichments among different lncRNA classes was determined using the *prop.test*

function in R.

Growth phenotypes of mutant cells

For a semi-quantitative analysis of cell growth, we used spot assays. After overnight pre-culture,

yeast cells were adjusted to the same OD value (~0.6). For each strain, 5 µl of six serial (five-fold)

dilutions were spotted onto YE plates and grown at 32°C.

Nucleosome profiling

Mononucleosomal DNA (MNase digested) from exponentially growing wild-type (*972 h⁻*) cells in

EMM2 was generated as reported (Lantermann et al. 2009). Two independent biological repeats were

performed. Sequencing libraries from MNase-digested DNA were prepared using the NEBNext

ChIP-Seq Library Prep Master Mix Set for Illumina (E6240S). Pair-end 50 bp reads were obtained

with an Illumina MiSeq sequencer at the Genomics and Genome Engineering Facility at the UCL

Cancer Institute. MNAse sequencing data was mapped using Bowtie2 (Langmead and Salzberg

2012). Nucleosome maps for visualisation were performed with nucwave (Quintales et al. 2015),

following the web recommendations (http://nucleosome.usal.es/nucwave/). Data were analysed

using the '*computeMatrix reference-point*' and '*heatmapper'* functions from the deeptools package

with transcription start sites as reference points (Ramírez et al. 2014).

Data availability

Sequencing data have been submitted to ArrayExpress and the European Nucleotide Archive under accession numbers PRJEB7403, E-MTAB-708, E-MTAB-2237, MTAB-1154, E-MTAB-1824 (RNA-seq; for sample accessions, see Supplemental Tables S1and S2) and PRJEB21376 (nucleosome profiling).

References

Anderson HE, Wardle J, Korkut S V., Murton HE, Lopez-Maury L, Bähler J, Whitehall SK. 2009.
The Fission Yeast HIRA Histone Chaperone Is Required for Promoter Silencing and the
Suppression of Cryptic Antisense Transcripts. *Mol Cell Biol* **29**: 5158–5167.

Ard R, Allshire RC, Marquardt S. 2017. Emerging Properties and Functional Consequences of
Noncoding Transcription. *Genetics* **207**: 357–367.

Ard R, Tong P, Allshire RC. 2014. Long non-coding RNA-mediated transcriptional interference of a
permease gene confers drug tolerance in fission yeast. *Nat Commun* **5**: 5576.

Atkinson SR, Marguerat S, Bähler J. 2012. Exploring long non-coding RNAs through sequencing.
Semin Cell Dev Biol **23**: 200–5.

Bähler J, Wise JA. 2017. Preparation of Total RNA from Fission Yeast. *Cold Spring Harb Protoc*
2017: pdb.prot091629.

Bähler J, Wu JQ, Longtine MS, Shah NG, McKenzie a, Steever a B, Wach a, Philippsen P, Pringle
JR. 1998. Heterologous modules for efficient and versatile PCR-based gene targeting in
Schizosaccharomyces pombe. *Yeast* **14**: 943–51.

Batista PJ, Chang HY. 2013. Long Noncoding RNAs: Cellular Address Codes in Development and
Disease. *Cell* **152**: 1298–1307.

Beaulieu YB, Kleinman CL, Landry-Voyer AM, Majewski J, Bachand F. 2012. Polyadenylation-
Dependent Control of Long Noncoding RNA Expression by the Poly(A)-Binding Protein Nuclear
1. *PLoS Genet* **8**: e1003078.

Bitton DA, Grallert A, Scutt PJ, Yates T, Li Y, Bradford JR, Hey Y, Pepper SD, Hagan IM, Miller
CJ. 2011. Programmed fluctuations in sense/antisense transcript ratios drive sexual differentiation
in S. pombe. *Mol Syst Biol* **7**: 559.

Bitton DA, Atkinson SR, Rallis C, Smith GC, Ellis DA, Chen YYC, Malecki M, Codlin S, Lemay JF,
Cotobal C, et al. 2015a. Widespread exon skipping triggers degradation by nuclear RNA
surveillance in fission yeast. *Genome Res* **25**: 884–896.

Bitton DA, Rallis C, Jeffares DC, Smith GC, Chen YYC, Codlin S, Marguerat S, Bähler J. 2014.

LaSSO, a strategy for genome-wide mapping of intronic lariats and branch points using RNA-seq. *Genome Res* **24**: 1169-1179.

Bitton DA, Schubert F, Dey S, Okoniewski M, Smith GC, Khadayate S, Pancaldi V, Wood V, Bähler J. 2015b. AnGeLi: A tool for the analysis of gene lists from fission yeast. *Front Genet* **6**: 1–9.

Bühler M, Spies N, Bartel DP, Moazed D. 2008. TRAMP-mediated RNA surveillance prevents spurious entry of RNAs into the Schizosaccharomyces pombe siRNA pathway. *Nat Struct Mol Biol* **15**: 1015–1023.

Cabili MN, Trapnell C, Goff L, Koziol M, Tazon-Vega B, Regev A, Rinn JL. 2011. Integrative annotation of human large intergenic noncoding RNAs reveals global properties and specific subclasses. *Genes Dev* **25**: 1915–1927.

Camblong J, Iglesias N, Fickentscher C, Dieppois G, Stutz F. 2007. Antisense RNA stabilization induces transcriptional gene silencing via histone deacetylation in S. cerevisiae. *Cell* **131**: 706–717.

Castel SE, Martienssen RA. 2013. RNA interference in the nucleus: roles for small RNAs in transcription, epigenetics and beyond. *Nat Rev Genet* **14**: 100–112.

Castelnuovo M, Zaugg JB, Guffanti E, Maffioletti A, Camblong J, Xu Z, Clauder-Münster S, Steinmetz LM, Luscombe NM, Stutz F. 2014. Role of histone modifications and early termination in pervasive transcription and antisense-mediated gene silencing in yeast. *Nucleic Acids Res* **42**: 4348.

Chen HM, Rosebrock AP, Khan SR, Futcher B, Leatherwood JK. 2012. Repression of meiotic genes by antisense transcription and by Fkh2 transcription factor in Schizosaccharomyces pombe. *PLoS One* **7**: e29917.

Clément-Ziza M, Marsellach FX, Codlin S, Papadakis MA, Reinhardt S, Rodríguez-López M, Martin S, Marguerat S, Schmidt A, Lee E, et al. 2014. Natural genetic variation impacts expression levels of coding, non-coding, and antisense transcripts in fission yeast. *Mol Syst Biol* **10**: 764.

Colin J, Candelli T, Porrua O, Boulay J, Zhu C, Lacroute F, Steinmetz LM, Libri D. 2014. Roadblock Termination by Reb1p Restricts Cryptic and Readthrough Transcription. *Mol Cell* **56**: 667–680.

de Andres-Pablo A, Morillon A, Wery M. 2017. LncRNAs, lost in translation or licence to regulate?

Curr Genet **63**: 29–33.

DeGennaro CM, Alver BH, Marguerat S, Stepanova E, Davis CP, Bähler J, Park PJ, Winston F. 2013.
Spt6 Regulates Intragenic and Antisense Transcription, Nucleosome Positioning, and Histone
Modifications Genome-Wide in Fission Yeast. *Mol Cell Biol* **33**: 4779–4792.

Derrien T, Johnson R, Bussotti G, Tanzer A, Djebali S, Tilgner H, Guernec G, Martin D, Merkel A,
Knowles DG, et al. 2012. The GENCODE v7 catalog of human long noncoding RNAs: Analysis
of their gene structure, evolution, and expression. *Genome Res* **22**: 1775–1789.

Ding D-Q, Okamasa K, Yamane M, Tsutsumi C, Haraguchi T, Yamamoto M, Hiraoka Y. 2012.
Meiosis-Specific Noncoding RNA Mediates Robust Pairing of Homologous Chromosomes in
Meiosis. *Science* **336**: 732-736.

Duncan CDS, Mata J. 2014. The translational landscape of fission-yeast meiosis and sporulation. *Nat
Struct Mol Biol* **21**: 641–647.

Dutrow N, Nix DA, Holt D, Milash B, Dalley B, Westbroek E, Parnell TJ, Cairns BR. 2008. Dynamic
transcriptome of Schizosaccharomyces pombe shown by RNA-DNA hybrid mapping. *Nat Genet*
40: 977–986.

Egan ED, Braun CR, Gygi SP, Moazed D. 2014. Post-transcriptional regulation of meiotic genes by a
nuclear RNA silencing complex. *RNA* **20**: 867–881.

Ehrensberger KM, Mason C, Corkins ME, Anderson C, Dutrow N, Cairns BR, Dalley B, Milash B,
Bird AJ. 2013. Zinc-dependent Regulation of the adh1 Antisense Transcript in Fission Yeast. *J
Biol Chem* **288**: 759–769.

Eser P, Wachutka L, Maier KC, Demel C, Boroni M, Iyer S, Cramer P, Gagneur J. 2016.
Determinants of RNA metabolism in the Schizosaccharomyces pombe genome. *Mol Syst Biol* **12**:
857.

Flicek P, Amode MR, Barrell D, Beal K, Billis K, Brent S, Carvalho-Silva D, Clapham P, Coates G,
Fitzgerald S, et al. 2014. Ensembl 2014. *Nucleic Acids Res* **42**: D749.

Frenk S, Oxley D, Houseley J. 2014. The Nuclear Exosome Is Active and Important during Budding
Yeast Meiosis ed. J. Bähler. *PLoS One* **9**: e107648.

Geisler S, Coller J. 2013. RNA in unexpected places: long non-coding RNA functions in diverse

cellular contexts. *Nat Rev Mol Cell Biol* **14**: 699–712.

Grzechnik P, Tan-Wong SM, Proudfoot NJ. 2014. Terminate and make a loop: regulation of transcriptional directionality. *Trends Biochem Sci* **39**: 319–327.

Guttman M, Amit I, Garber M, French C, Lin MF, Feldser D, Huarte M, Zuk O, Carey BW, Cassady JP, et al. 2009. Chromatin signature reveals over a thousand highly conserved large non-coding RNAs in mammals. *Nature* **458**: 223–227.

Guttman M, Rinn JL. 2012. Modular regulatory principles of large non-coding RNAs. *Nature* **482**: 339–46.

Haimovich G, Medina D a, Causse SZ, Garber M, Millán-Zambrano G, Barkai O, Chávez S, Pérez-Ortín JE, Darzacq X, Choder M. 2013. Gene expression is circular: factors for mRNA degradation also foster mRNA synthesis. *Cell* **153**: 1000–11.

Hangauer MJ, Vaughn IW, McManus MT. 2013. Pervasive Transcription of the Human Genome Produces Thousands of Previously Unidentified Long Intergenic Noncoding RNAs. *PLOS Genet* **9**: 1–13.

Hansen TB, Jensen TI, Clausen BH, Bramsen JB, Finsen B, Damgaard CK, Kjems J. 2013. Natural RNA circles function as efficient microRNA sponges. *Nature* **495**: 384–8.

Harigaya Y, Tanaka H, Yamanaka S, Tanaka K, Watanabe Y, Tsutsumi C, Chikashige Y, Hiraoka Y, Yamashita A, Yamamoto M. 2006. Selective elimination of messenger RNA prevents an incidence of untimely meiosis. *Nature* **442**: 45–50.

Harrison BR, Yazgan O, Krebs JE. 2009. Life without RNAi: noncoding RNAs and their functions in Saccharomyces cerevisiaeThis paper is one of a selection of papers published in this Special Issue, entitled 30th Annual International Asilomar Chromatin and Chromosomes Conference, and has undergon. *Biochem Cell Biol* **87**: 767–779.

Hasan A, Cotobal C, Duncan CDS, Mata J. 2014. Systematic Analysis of the Role of RNA-Binding Proteins in the Regulation of RNA Stability ed. G.P. Copenhaver. *PLoS Genet* **10**: e1004684.

Hennig BP, Bendrin K, Zhou Y, Fischer T. 2012. Chd1 chromatin remodelers maintain nucleosome organization and repress cryptic transcription. *EMBO Rep* **13**: 997-1003.

Hirota K, Miyoshi T, Kugou K, Hoffman CS, Shibata T, Ohta K. 2008. Stepwise chromatin

remodelling by a cascade of transcription initiation of non-coding RNAs. *Nature* **456**: 130–134.

Hon C-C, Ramilowski JA, Harshbarger J, Bertin N, Rackham OJL, Gough J, Denisenko E, Schmeier S, Poulsen TM, Severin J, et al. 2017. An atlas of human long non-coding RNAs with accurate 5′ ends. *Nature* **543**: 199–204.

Houseley J, Rubbi L, Grunstein M, Tollervey D, Vogelauer M. 2008. A ncRNA Modulates Histone Modification and mRNA Induction in the Yeast {GAL} Gene Cluster. *Mol Cell* **32**: 685–695.

Houseley J, Tollervey D. 2009. The Many Pathways of RNA Degradation. *Cell* **136**: 763–776.

Jandura A, Krause HM. 2017. The New RNA World: Growing Evidence for Long Noncoding RNA Functionality. *Trends Genet* **33**: 665–676.

Jeffares DC, Rallis C, Rieux A, Speed D, Převorovský M, Mourier T, Marsellach FX, Iqbal Z, Lau W, Cheng TMK, et al. 2015. The genomic and phenotypic diversity of Schizosaccharomyces pombe. *Nat Genet* **47**: 235–241.

Jensen TH, Jacquier A, Libri D. 2013. Dealing with Pervasive Transcription. *Mol Cell* **52**: 473–484.

Joh RI, Khanduja JS, Calvo IA, Mistry M, Palmieri CM, Savol AJ, Sui SJH, Sadreyev RI, Aryee MJ, Motamedi M. 2016. Survival in Quiescence Requires the Euchromatic Deployment of Clr4/SUV39H by Argonaute-Associated Small RNAs. *Mol Cell* **64**: 1088–1101.

Kilchert C, Wittmann S, Vasiljeva L. 2016. The regulation and functions of the nuclear RNA exosome complex. *Nat Rev Mol Cell Biol* **17**: 227–239.

Kumar L, E. Futschik M. 2007. Mfuzz: A software package for soft clustering of microarray data. *Bioinformation* **2**: 5–7.

Lackner DH, Beilharz TH, Marguerat S, Mata J, Watt S, Schubert F, Preiss T, Bähler J. 2007. A Network of Multiple Regulatory Layers Shapes Gene Expression in Fission Yeast. *Mol Cell* **26**.

Langmead B, Salzberg SL. 2012. Fast gapped-read alignment with Bowtie 2. *Nat Meth* **9**: 357–359.

Lantermann A, Strålfors A, Fagerström-Billai F, Korber P, Ekwall K. 2009. Genome-wide mapping of nucleosome positions in Schizosaccharomyces pombe. *Methods* **48**: 218–225.

Lantermann AB, Straub T, Strålfors A, Yuan G-C, Ekwall K, Korber P. 2010. Schizosaccharomyces pombe genome-wide nucleosome mapping reveals positioning mechanisms distinct from those of Saccharomyces cerevisiae. *Nat Struct Mol Biol* **17**: 251–7.

Lee NN, Chalamcharla VR, Reyes-Turcu F, Mehta S, Zofall M, Balachandran V, Dhakshnamoorthy J, Taneja N, Yamanaka S, Zhou M, et al. 2013. Mtr4-like protein coordinates nuclear RNA processing for heterochromatin assembly and for telomere maintenance. *Cell* **155**: 1061–1074.

Lemay J-F, Larochelle M, Marguerat S, Atkinson S, Bähler J, Bachand F. 2014. The RNA exosome promotes transcription termination of backtracked RNA polymerase II. *Nat Struct Mol Biol* **21**: 919–926.

Lemay J-F, Marguerat S, Larochelle M, Liu X, van Nues R, Hunyadkürti J, Hoque M, Tian B, Granneman S, Bähler J, et al. 2016. The Nrd1-like protein Seb1 coordinates cotranscriptional 3′ end processing and polyadenylation site selection. *Genes Dev* **30**: 1558-1572.

Lemay JF, D'Amours A, Lemieux C, Lackner DH, St-Sauveur VG, Bähler J, Bachand F. 2010. The Nuclear Poly(A)-Binding Protein Interacts with the Exosome to Promote Synthesis of Noncoding Small Nucleolar RNAs. *Mol Cell* **37**: 34–45.

Lemieux C, Marguerat S, Lafontaine J, Barbezier N, Bähler J, Bachand F. 2011. A Pre-mRNA degradation pathway that selectively targets intron-containing genes requires the nuclear poly(A)-binding protein. *Mol Cell* **44**: 108-119

Leong HS, Dawson K, Wirth C, Li Y, Connolly Y, Smith DL, Wilkinson CRM, Miller CJ. 2014. A global non-coding RNA system modulates fission yeast protein levels in response to stress. *Nat Commun* **5**: 3947.

Li H, Hou J, Bai L, Hu C, Tong P, Kang Y, Zhao X, Shao Z. 2015. Genome-wide analysis of core promoter structures in Schizosaccharomyces pombe with DeepCAGE. *RNA Biol* **12**: 525–537.

Li X, Manley JL. 2006. Cotranscriptional processes and their influence on genome stability. *Genes Dev* **20**: 1838–1847.

Liu X, Hoque M, Larochelle M, Lemay J-F, Yurko N, Manley JL, Bachand F, Tian B. 2017. Comparative analysis of alternative polyadenylation in S. cerevisiae and S. pombe. *Genome Res* **27**: 1685–1695.

Love MI, Huber W, Anders S. 2014. Moderated estimation of fold change and dispersion for RNA-seq data with DESeq2. *Genome Biol* **15**: 550.

Malabat C, Feuerbach F, Ma L, Saveanu C, Jacquier A. 2015. Quality control of transcription start

site selection by nonsense-mediated-mRNA decay ed. T.H. Jensen. *Elife* **4**: e06722.

Marguerat S, Schmidt A, Codlin S, Chen W, Aebersold R, Bähler J. 2012. Quantitative analysis of fission yeast transcriptomes and proteomes in proliferating and quiescent cells. *Cell* **151**: 671–683.

Marquardt S, Hazelbaker DZ, Buratowski S. 2011. Distinct RNA degradation pathways and 3' extensions of yeast non-coding RNA species. *Transcription* **2**: 145–154.

Mata J. 2013. Genome-wide mapping of polyadenylation sites in fission yeast reveals widespread alternative polyadenylation. *RNA Biol* **10**: 1407–1414.

Mata J, Lyne R, Burns G, Bähler J. 2002. The transcriptional program of meiosis and sporulation in fission yeast. *Nat Genet* **32**: 143–147.

Mattick JS, Rinn JL. 2015. Discovery and annotation of long noncoding RNAs. *Nat Struct Mol Biol* **22**: 5–7.

McDowall MD, Harris M a., Lock a., Rutherford K, Staines DM, Bähler J, Kersey PJ, Oliver SG, Wood V. 2014. PomBase 2015: updates to the fission yeast database. *Nucleic Acids Res* **43**: D656–D661.

McPheeters DS, Cremona N, Sunder S, Chen H-M, Averbeck N, Leatherwood J, Wise JA. 2009. A Complex Gene Regulatory Mechanism that Operates at the Nexus of Multiple RNA Processing Decisions. *Nat Struct Mol Biol* **16**: 255–264.

Mellor J, Woloszczuk R, Howe FS. 2016. The Interleaved Genome. *Trends Genet* **32**: 57–71.

Meola N, Domanski M, Karadoulama E, Chen Y, Gentil C, Pultz D, Vitting-Seerup K, Lykke-Andersen S, Andersen JS, Sandelin A, et al. 2016. Identification of a Nuclear Exosome Decay Pathway for Processed Transcripts. *Mol Cell* **64**: 520–533.

Mercer TR, Mattick JS. 2013. Structure and function of long noncoding RNAs in epigenetic regulation. *Nat Struct Mol Biol* **20**: 300–7.

Mukherjee N, Calviello L, Hirsekorn A, de Pretis S, Pelizzola M, Ohler U. 2017. Integrative classification of human coding and noncoding genes through RNA metabolism profiles. *Nat Struct Mol Biol* **24**: 86–96.

Neil H, Malabat C, d'Aubenton-Carafa Y, Xu Z, Steinmetz LM, Jacquier A. 2009. Widespread bidirectional promoters are the major source of cryptic transcripts in yeast. *Nature* **457**: 1038–

1042.

Ni T, Tu K, Wang Z, Song S, Wu H, Xie B, Scott KC, Grewal SI, Gao Y, Zhu J. 2010. The

prevalence and regulation of antisense transcripts in Schizosaccharomyces pombe. *PLoS One* **5**:

e15271.

Oda A, Takemata N, Hirata Y, Miyoshi T, Suzuki Y, Sugano S, Ohta K. 2015. Dynamic transition of

transcription and chromatin landscape during fission yeast adaptation to glucose starvation. *Genes*

to Cells **20**: 392–407.

Pancaldi V, Schubert F, Bähler J. 2010. Meta-analysis of genome regulation and expression

variability across hundreds of environmental and genetic perturbations in fission yeast. *Mol*

Biosyst **6**: 543-552.

Pauli A, Valen E, Lin MF, Garber M, Vastenhouw NL, Levin JZ, Fan L, Sandelin A, Rinn JL, Regev

A, et al. 2012. Systematic identification of long noncoding RNAs expressed during zebrafish

embryogenesis. *Genome Res* **22**: 577–591.

Pelechano V, Steinmetz LM. 2013. Gene regulation by antisense transcription. *Nat Rev Genet* **14**:

880–893.

Perocchi F, Xu Z, Clauder-Münster S, Steinmetz LM. 2007. Antisense artifacts in transcriptome

microarray experiments are resolved by actinomycin D. *Nucleic Acids Res* **35**: e128.

Pointner J, Persson J, Prasad P, Norman-Axelsson U, Strålfors A, Khorosjutina O, Krietenstein N,

Peter Svensson J, Ekwall K, Korber P. 2012. CHD1 remodelers regulate nucleosome spacing

in vitro and align nucleosomal arrays over gene coding regions in S.

pombe. *EMBO J* **31**: 4388-4403.

Preker P, Nielsen J, Kammler S, Lykke-Andersen S, Christensen MS, Mapendano CK, Schierup MH,

Jensen TH. 2008. RNA Exosome Depletion Reveals Transcription Upstream of Active Human

Promoters. *Science* **322**: 1851-1854.

Quinn JJ, Chang HY. 2016. Unique features of long non-coding RNA biogenesis and function. *Nat*

Rev Genet **17**: 47–62.

Quintales L, Vázquez E, Antequera F. 2015. Comparative analysis of methods for genome-wide

nucleosome cartography. *Brief Bioinform* **16**: 576.

Ramírez F, Dündar F, Diehl S, Grüning BA, Manke T. 2014. deepTools: a flexible platform for exploring deep-sequencing data. *Nucleic Acids Res* **42**: W187.

Rhind N, Chen Z, Yassour M, Thompson D a, Haas BJ, Habib N, Wapinski I, Roy S, Lin MF, Heiman DI, et al. 2011. Comparative functional genomics of the fission yeasts. *Science* **332**: 930–6.

Rinn JL, Chang HY. 2012. Genome Regulation by Long Noncoding RNAs. *Annu Rev Biochem* **81**: 145–166.

Rodríguez-Gabriel MA, Watt S, Bähler J, Russell P. 2006. Upf1, an RNA helicase required for nonsense-mediated mRNA decay, modulates the transcriptional response to oxidative stress in fission yeast. *Mol Cell Biol* **26**: 6347-6356.

Schlackow M, Marguerat S, Proudfoot NJ, Bähler J, Erban R, Gullerova M. 2013. Genome-wide analysis of poly(A) site selection in Schizosaccharomyces pombe. *RNA* **19**: 1617-1631.

Schlackow M, Nojima T, Gomes T, Dhir A, Carmo-Fonseca M, Proudfoot NJ. 2017. Distinctive Patterns of Transcription and RNA Processing for Human lincRNAs. *Mol Cell* **65**: 25–38.

Schmidt M-J, West S, Norbury CJ. 2011. The human cytoplasmic RNA terminal U-transferase ZCCHC11 targets histone mRNAs for degradation. *RNA* **17**: 39–44.

Schulz D, Schwalb B, Kiesel A, Baejen C, Torkler P, Gagneur J, Soeding J, Cramer P. 2013. Transcriptome Surveillance by Selective Termination of Noncoding RNA Synthesis. *Cell* **155**: 1075–1087.

Shah S, Wittmann S, Kilchert C, Vasiljeva L. 2014. lncRNA recruits RNAi and the exosome to dynamically regulate pho1 expression in response to phosphate levels in fission yeast. *Genes Dev* **28**: 231–244.

Shetty A, Kallgren SP, Demel C, Maier KC, Spatt D, Alver BH, Cramer P, Park PJ, Winston F. 2017. Spt5 Plays Vital Roles in the Control of Sense and Antisense Transcription Elongation. *Mol Cell* **66**: 77–88.e5.

Shim YS, Choi Y, Kang K, Cho K, Oh S, Lee J, Grewal SIS, Lee D. 2012. Hrp3 controls nucleosome positioning to suppress non-coding transcription in eu- and heterochromatin. *EMBO J* **31**: 4375-4387.

Slater GSC, Birney E. 2005. Automated generation of heuristics for biological sequence comparison. *BMC Bioinformatics* **6**: 31.

Smialowska A, Djupedal I, Wang J, Kylsten P, Swoboda P, Ekwall K. 2014. RNAi mediates post-transcriptional repression of gene expression in fission yeast Schizosaccharomyces pombe. *Biochem Biophys Res Commun* **444**: 254–259.

St-André O, Lemieux C, Perreault A, Lackner DH, Bähler J, Bachand F. 2010. Negative regulation of meiotic gene expression by the nuclear poly(a)-binding protein in fission yeast. *J Biol Chem* **285**.

St. Laurent G, Wahlestedt C, Kapranov P. 2015. The Landscape of long noncoding RNA classification. *Trends Genet* **31**: 239–251.

Sugiyama T, Sugioka-Sugiyama R. 2011. Red1 promotes the elimination of meiosis-specific mRNAs in vegetatively growing fission yeast. *EMBO J* **30**: 1027–1039.

Sun M, Schwalb B, Pirkl N, Maier KC, Schenk A, Failmezger H, Tresch A, Cramer P. 2017. Global Analysis of Eukaryotic mRNA Degradation Reveals Xrn1-Dependent Buffering of Transcript Levels. *Mol Cell* **52**: 52–62.

Szankasi P, Smith GR. 1996. Requirement of S. pombe exonuclease II, a homologue of S. cerevisiae Sep1, for normal mitotic growth and viability. *Curr Genet* **30**: 284–293.

Touat-Todeschini L, Shichino Y, Dangin M, Thierry-Mieg N, Gilquin B, Hiriart E, Sachidanandam R, Lambert E, Brettschneider J, Reuter M, et al. 2017. Selective termination of lncRNA transcription promotes heterochromatin silencing and cell differentiation. *EMBO J* **36**: 2626-2641.

Tuck AC, Tollervey D. 2013. A Transcriptome-wide Atlas of RNP Composition Reveals Diverse Classes of mRNAs and lncRNAs. *Cell* **154**: 996–1009.

Tudek A, Porrua O, Kabzinski T, Lidschreiber M, Kubicek K, Fortova A, Lacroute F, Vanacova S, Cramer P, Stefl R, et al. 2014. Molecular Basis for Coordinating Transcription Termination with Noncoding RNA Degradation. *Mol Cell* **55**: 467–481.

Ulitsky I, Bartel DP. 2013. lincRNAs: Genomics, Evolution, and Mechanisms. *Cell* **154**: 26–46.

van Dijk EL, Chen CL, d/'Aubenton-Carafa Y, Gourvennec S, Kwapisz M, Roche V, Bertrand C, Silvain M, Legoix-Ne P, Loeillet S, et al. 2011. XUTs are a class of Xrn1-sensitive antisense regulatory non-coding RNA in yeast. *Nature* **475**: 114–117.

Volpe TA, Kidner C, Hall IM, Teng G, Grewal SIS, Martienssen RA. 2002. Regulation of Heterochromatic Silencing and Histone H3 Lysine-9 Methylation by RNAi. *Science* **297**: 1833–1837.

Wang G-Z, Lercher MJ, Hurst LD. 2011. Transcriptional coupling of neighboring genes and gene expression noise: evidence that gene orientation and noncoding transcripts are modulators of noise. *Genome Biol Evol* **3**: 320–31.

Wang S-W, Stevenson AL, Kearsey SE, Watt S, Bähler J. 2008. Global role for polyadenylation-assisted nuclear RNA degradation in posttranscriptional gene silencing. *Mol Cell Biol* **28**: 656-665.

Wery M, Descrimes M, Vogt N, Dallongeville A-S, Gautheret D, Morillon A. 2016. Nonsense-Mediated Decay Restricts LncRNA Levels in Yeast Unless Blocked by Double-Stranded RNA Structure. *Mol Cell* **61**: 379–392.

Wery M, Gautier C, Descrimes M, Yoda M, Vennin-Rendos H, Migeot V, Gautheret D, Hermand D, Morillon A. 2018. Native Elongating Transcript Sequencing reveals global anti-correlation between sense and antisense nascent transcription in fission yeast. *RNA* **24**:196-208 .

Wilhelm BT, Marguerat S, Watt S, Schubert F, Wood V, Goodhead I, Penkett CJ, Rogers J, Bähler J. 2008. Dynamic repertoire of a eukaryotic transcriptome surveyed at single-nucleotide resolution. *Nature* **453**: 1239–43.

Wittmann S, Renner M, Watts BR, Adams O, Huseyin M, Baejen C, El Omari K, Kilchert C, Heo D-H, Kecman T, et al. 2017. The conserved protein Seb1 drives transcription termination by binding RNA polymerase II and nascent RNA. **8**: 14861.

Wlotzka W, Kudla G, Granneman S, Tollervey D. 2011. The nuclear RNA polymerase II surveillance system targets polymerase III transcripts. *EMBO J* **30**: 1790 LP-1803.

Wolf J, Passmore LA. 2014. mRNA deadenylation by Pan2–Pan3. *Biochem Soc Trans* **42**: 184-187.

Wood V, Harris M a., McDowall MD, Rutherford K, Vaughan BW, Staines DM, Aslett M, Lock A, Bähler J, Kersey PJ, et al. 2012. PomBase: A comprehensive online resource for fission yeast. *Nucleic Acids Res* **40**: 695–699.

Wu X, Sharp PA. 2013. Divergent Transcription: A Driving Force for New Gene Origination? *Cell* **155**: 990–996.

Xu Z, Wei W, Gagneur J, Perocchi F, Clauder-Munster S, Camblong J, Guffanti E, Stutz F, Huber W, Steinmetz LM. 2009. Bidirectional promoters generate pervasive transcription in yeast. *Nature* **457**: 1033–1037.

Yamanaka S, Mehta S, Reyes-Turcu FE, Zhuang F, Fuchs RT, Rong Y, Robb GB, Grewal SIS. 2013. RNAi triggered by specialized machinery silences developmental genes and retrotransposons. *Nature* **493**: 557–560.

Yamanaka S, Yamashita A, Harigaya Y, Iwata R, Yamamoto M. 2010. Importance of polyadenylation in the selective elimination of meiotic mRNAs in growing S. pombe cells. *EMBO J* **29**: 2173-2181.

Yamashita A, Shichino Y, Yamamoto M. 2016. The long non-coding RNA world in yeasts. *Biochim Biophys Acta - Gene Regul Mech* **1859**: 147–154.

Zhang K, Fischer T, Porter RL, Dhakshnamoorthy J, Zofall M, Zhou M, Veenstra T, Grewal SIS. 2011. Clr4/Suv39 and RNA Quality Control Factors Cooperate to Trigger RNAi and Suppress Antisense RNA. *Science* **331**: 1624 LP-1627.

Zhou Y, Zhu J, Schermann G, Ohle C, Bendrin K, Sugioka-Sugiyama R, Sugiyama T, Fischer T. 2015. The fission yeast MTREC complex targets CUTs and unspliced pre-mRNAs to the nuclear exosome. *Nat Commun* **6**: 7050.

Zofall M, Fischer T, Zhang K, Zhou M, Cui B, Veenstra TD, Grewal SIS. 2009. Histone H2A.Z cooperates with RNAi and heterochromatin factors to suppress antisense RNAs. *Nature* **461**: 419–422.

Table 1. Data of actively translated lncRNA classes

lncRNA	Total lncRNAs	Translated lncRNAs ≥1 / ≥10 codons	Proportion translated: ≥1 / ≥10 codons
All	7348	557 / 256	7.6% / 3.5%
Novel	5775	148 / 66	2.6% / 1.1%
CUTs	2732	210 / 85	7.7% / 3.1%
DUTs	1392	40 / 17	2.9% / 1.2%
XUTs	1116	60 /33	5.4% / 3.0%
Bidirectional	1577	224 / 98	14.2% / 6.2%
Antisense	4474	215 / 104	4.8% / 2.3%
Intergenic	1189	86 / 42	7.2% / 3.5%
Sense	108	32 / 12	29.6% / 11.1%

FIGURE LEGENDS

Figure 1. Hierarchical clustering of gene expression in different RNA-processing mutants and physiological conditions. Expression profiles are shown for (**A**) all 5177 mRNAs, (**B**) 1573 annotated lncRNAs, and (**C**) 5775 novel, unannotated lncRNAs. Changes in RNA levels in response to the different genetic and physiological conditions (indicated at bottom) relative to control cells grown in minimal medium are color-coded as shown in the colour-legend at bottom right (log2 expression ratios). The *rrp6* and *exo2* samples indicated by asterisks has been depleted for rRNA instead of polyA purification used for all other samples. Data obtained from these two types of RNA-seq libraries are compared in Supplemental Figure S2b. Details on strains and conditions are provided in Supplemental Tables S1 and S2, and all expression data are provided in Supplemental Table S3.

Figure 2. Histograms showing numbers and proportions of induced (orange), repressed (blue) and all other (grey) transcripts for the different RNA classes as indicated. Differentially expressed genes were defined as those being ≥2-fold induced (mean of two biological repeats) or repressed and showing significant changes ($p < 0.05$) compared to reference as determined by DESeq2.

Figure 3. Gene expression in major groups of genetic and environmental conditions. (**A**) Left graph: box plot of expression ratios (condition relative to control) of all mRNAs, annotated and novel lncRNAs in nuclear exosome (*rrp6Δ, rrp6-ts*), RNAi (*ago1Δ, dcr1Δ, rdp1Δ*) and cytoplasmic exonuclease (*exo2Δ*) mutants. Right graph: as left but for quiescence, stationary phase and meiosis conditions. The horizontal dashed lines indicate 2-fold induction and repression.

(**B**) As in panel **A**, but for expression levels (RPKM scores). All expression data are

provided in Supplemental Table S3.

Figure 4. Classification of lncRNAs into CUTs, DUTs and XUTs.

(**A**) The lncRNAs significantly induced (DESeq2; adjusted p ≤0.05) in *rrp6Δ*, *dcr1Δ* or *exo2Δ*

mutants were clustered into CUTs, DUTs and XUTs, respectively, using the Mfuzz R

package (default parameters, 3 clusters specified). The clustering shows the 5586 uniquely

classified lncRNAs after filtering those with a membership score <0.7. The red/blue colours

indicate the mean RPKM values in the 3 mutants as indicated, scaled by subtracting the

mean of the row and division by the standard deviation of the row (z-score). The assigned

clusters are indicated at left.

(**B**) Box plots of RPKM values (log2) of all CUTs (left), DUTs (middle) and XUTs (right) in

control (MM) and mutant cells as indicated. The data for the biological repeats 1 and 2 are

plotted separately.

(**C**) Hierarchical clustering of genetic conditions for all CUTs, DUTs and XUTs as indicated.

Changes in RNA levels in response to the different genetic conditions (indicated at bottom)

relative to control cells grown in minimal medium are color-coded as shown in the legend at

bottom right (log2 expression ratios). All expression and classification data are provided in

Supplemental Table S3.

Figure 5. Analyses of lncRNAs by positions relative to mRNAs.

(**A**) We grouped the annotated and novel lncRNAs into three main positional types as

represented schematically: 1577 Bidirectional, 4474 Antisense and 1189 Intergenic RNAs,

leaving only 108 lncRNAs (105 annotated, 3 novel) that overlapped mRNAs in sense

direction (Materials and methods). Pie charts of the corresponding proportions of CUTs,

DUTs, XUTs and other lncRNAs are provided beneath each positional type, and also for all

annotated and known lncRNAs. Significantly enriched slices are indicated with asterisks (*R*

prop.test function, p <10^{-6}).

(**B**) Pie charts of the proportions of Bidirectional, Antisense, Intergenic and Sense lncRNAs

for all (annotated and known) lncRNAs, and among the CUTs, DUTs and XUTs.

Significantly enriched slices are indicated with asterisks (*R prop.test function*, p <10^{-4}).

(**C**) Pearson correlation coefficients for RPKM expression data of each Bidirectional

lncRNA-mRNA pair (left) and each Antisense lncRNA-mRNA pair (right). The correlation

data are shown separately for all genetic and physiological conditions as indicated on X-

axes. For Antisense lncRNAs, the difference between the distributions in genetic *vs*

physiological conditions is highly significant ($P_{Wilcoxon}$ = 4.6e^{-170}). All classification data are

provided in Supplemental Table S5.

Figure 6. Expression patterns of Bidirectional, Antisense and Intergenic lncRNAs.

(**A**) Histograms showing the numbers and proportions of the induced (orange), repressed

(blue) and all other (grey) transcripts for the different lncRNA classes as indicated.

Differentially expressed genes were defined as those being >2-fold induced (average of two

biological repeats) or repressed and showing significant changes (p <0.05) compared to

reference as determined by DESeq2.

(**B**) Hierarchical clustering of physiological conditions for different lncRNA classes as

indicated. Changes in RNA levels in response to the different physiological conditions

(indicated at bottom) relative to control cells grown in minimal medium are color-coded as

shown in the legend at bottom (log2 expression ratios). Hierarchical clustering of

physiological conditions for CUTs, DUTs and XUTs is shown in Supplemental Figure S4. All

expression and classification data are provided in Supplemental Tables S3 and S5.

Figure 7. Nucleosome patterns for coding and non-coding transcribed regions.

Nucleosome profiling data for all mRNA loci (left), 509 Bidirectional lncRNA loci and 1119

Intergenic lncRNA loci (right) in proliferating wild-type cells. Bidirectional lncRNA loci that

overlap mRNAs in antisense direction were not included. We omitted 70 intergenic lncRNA

loci that showed unusually high histone occupancies (Supplemental Table S8); these loci

are mostly located in centromeric or subtelomeric regions. The top graphs show average

nucleosome profiles for the different types of transcribed regions, aligned to the transcription

start sites (TSS). The lower graphs show heatmaps for the first two kilobases of all

transcribed regions analysed, ordered by transcript length from top (longest RNAs) to bottom

(shortest RNAs). Sequencing scores are color-coded as shown in legend at bottom right.

Figure 1
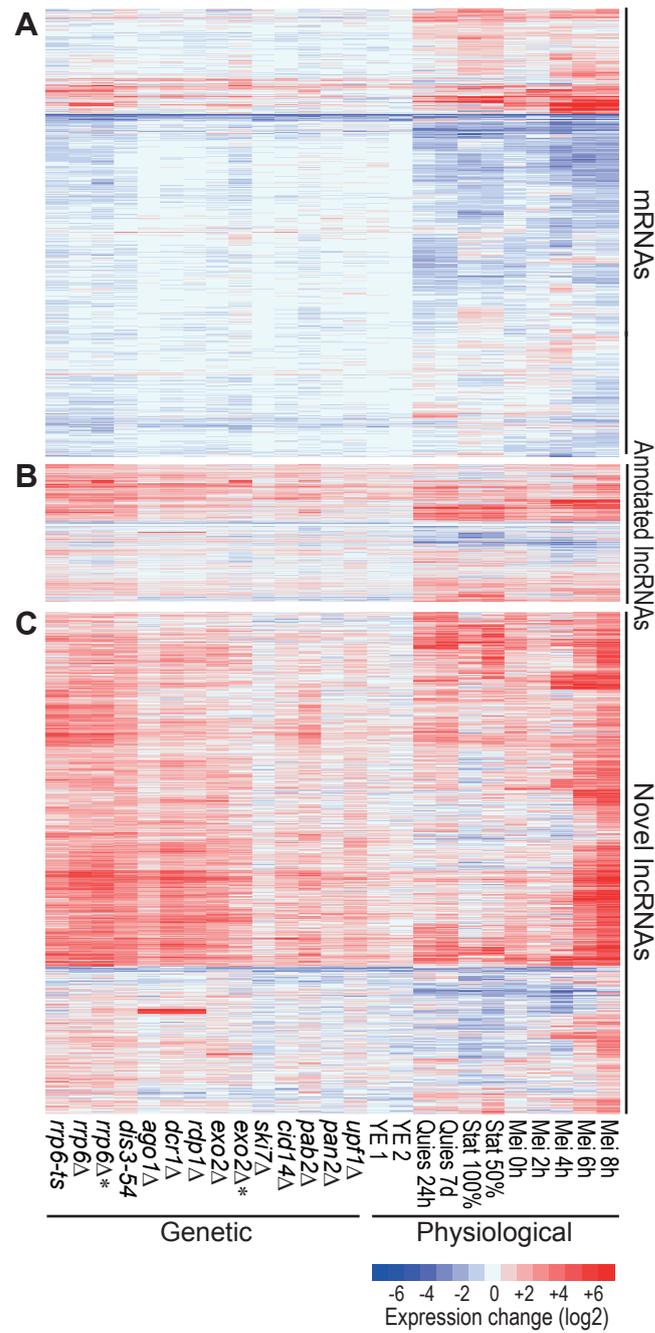
Figure 2
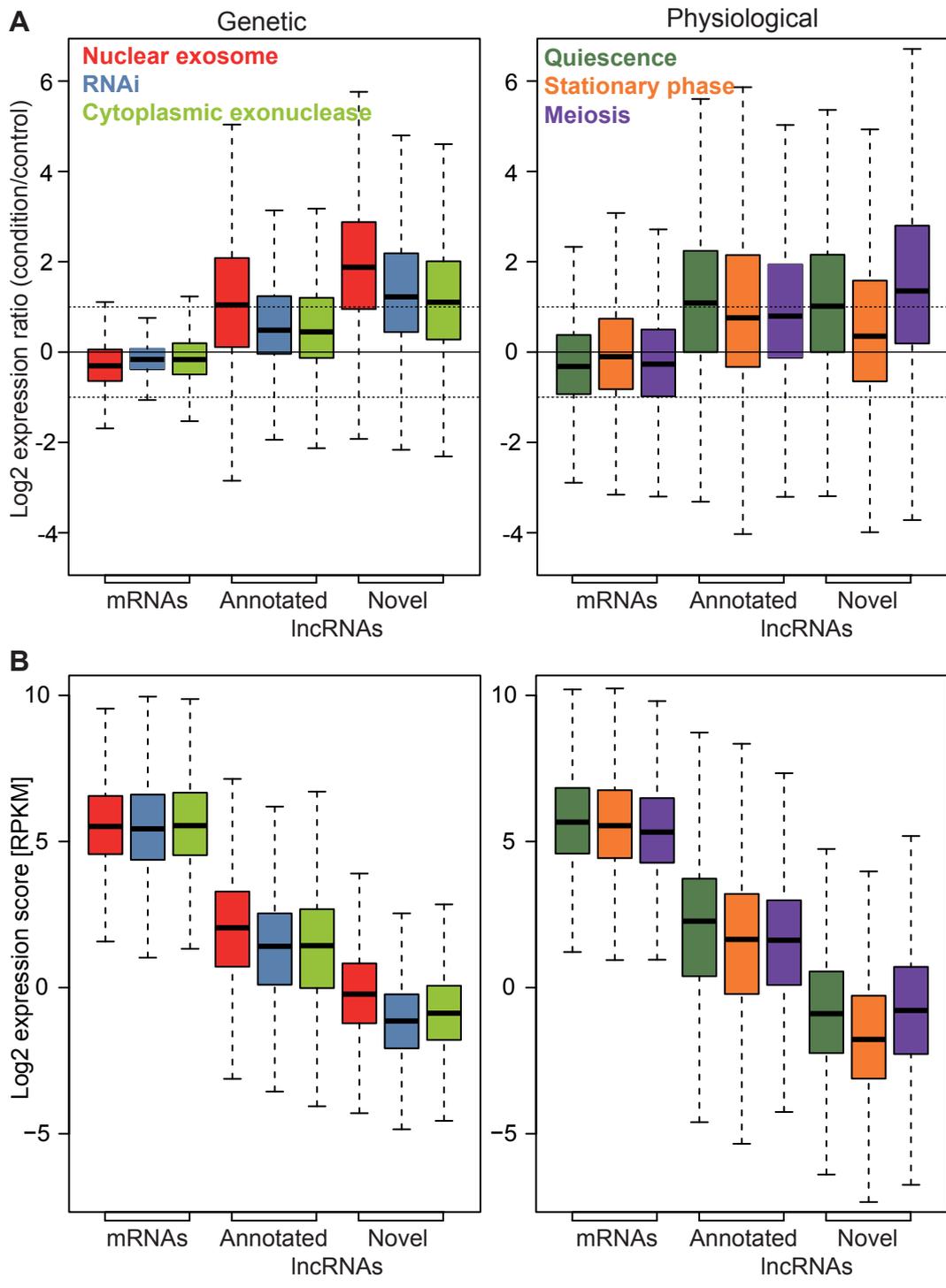
Figure 2
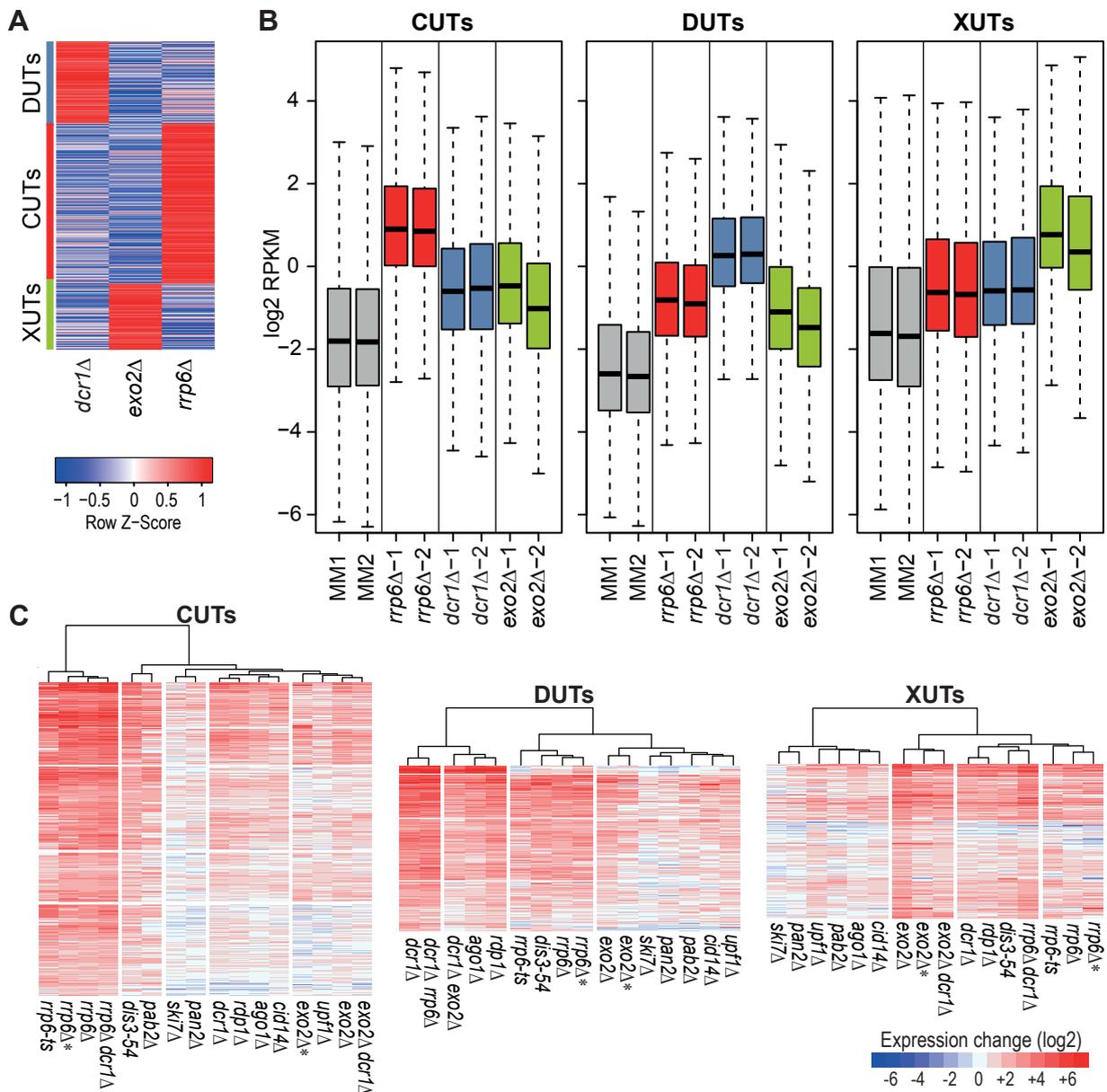
Figure 3

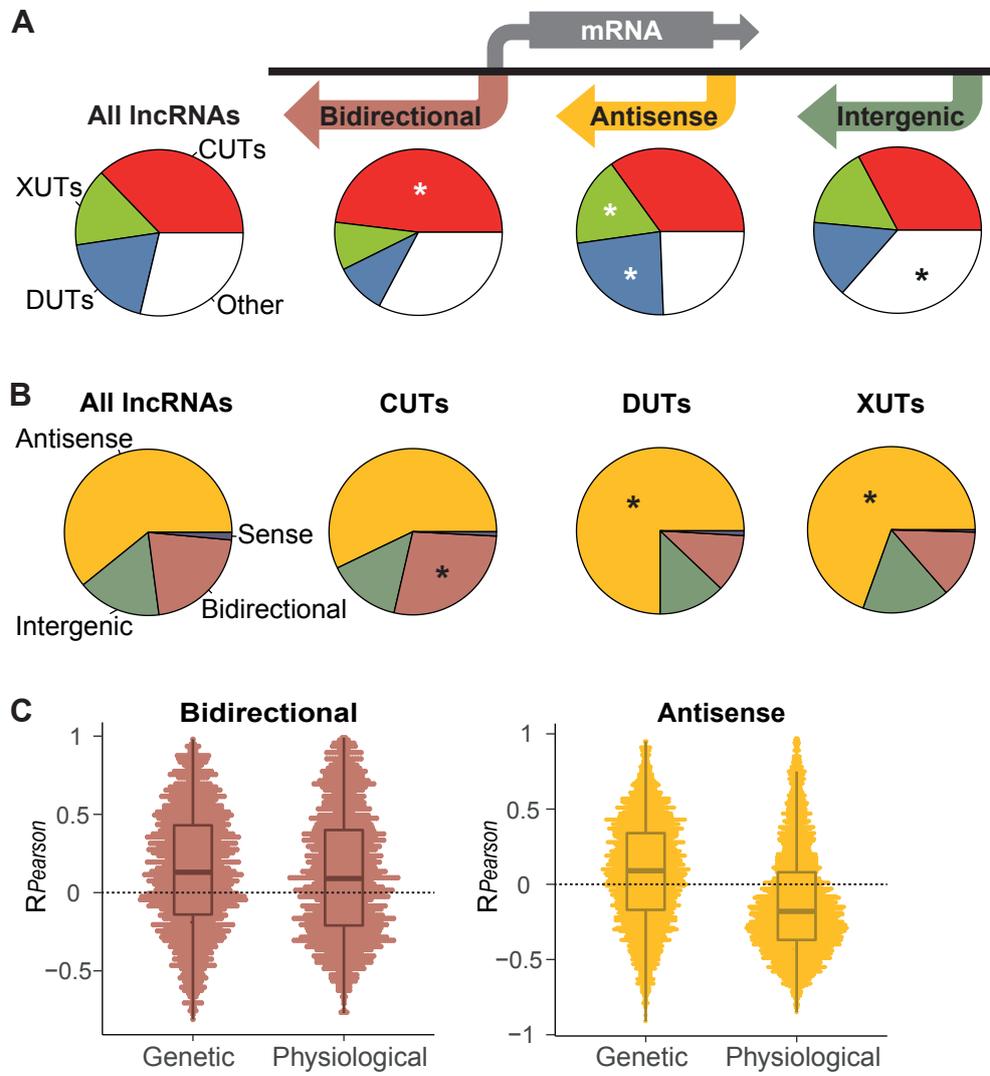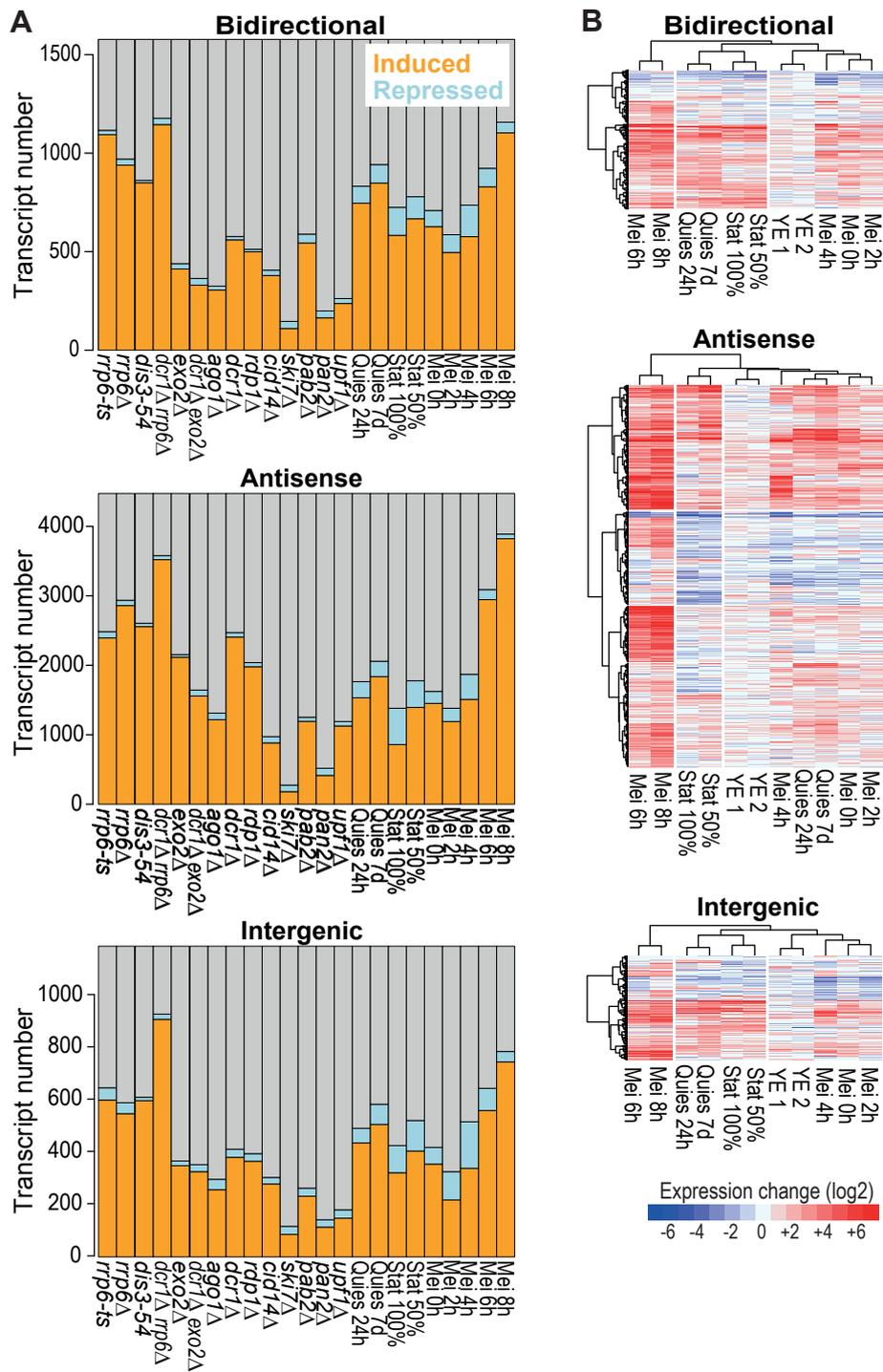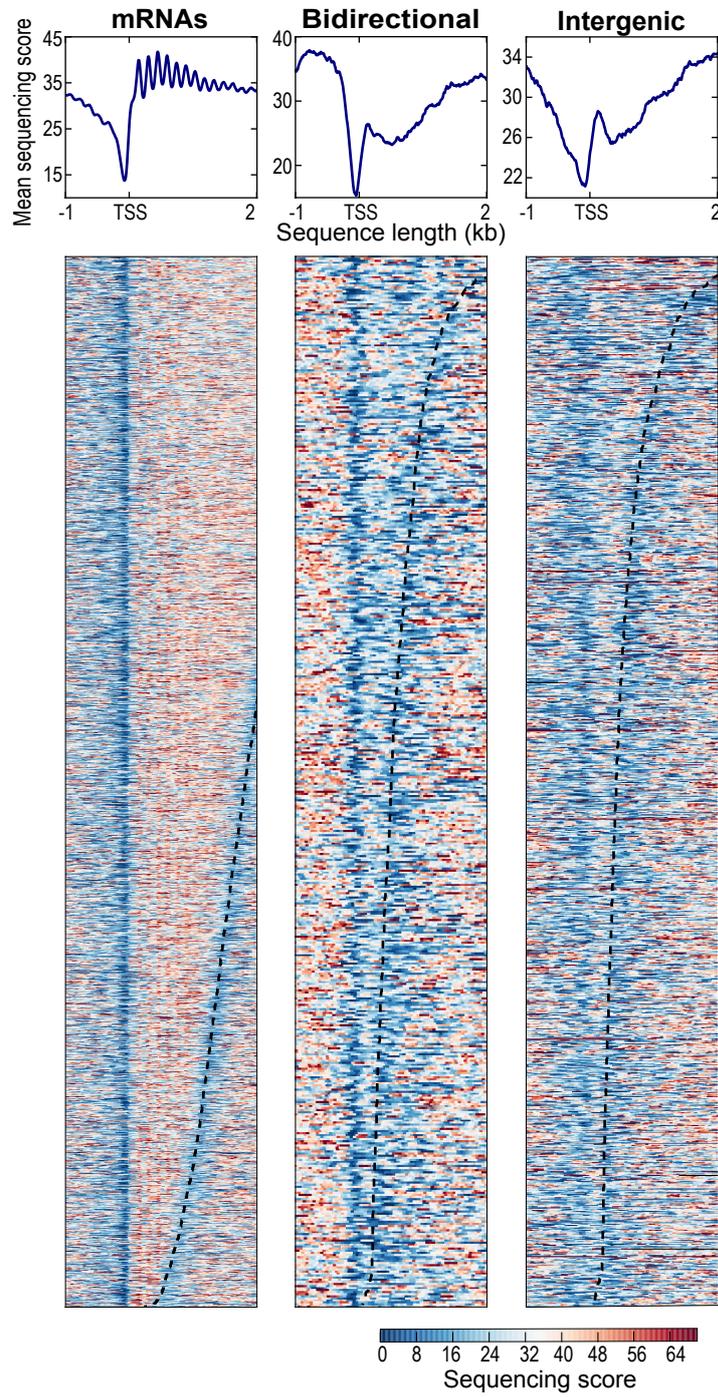# Figure 4

Figure 5

Figure 6

Figure 7

RNA

A PUBLICATION OF THE RNA SOCIETY

Long non-coding RNA repertoire and targeting by nuclear exosome, cytoplasmic exonuclease and RNAi in fission yeast

Sophie Atkinson, Samuel Marguerat, Danny Bitton, et al.

Supplemental Material	http://rnajournal.cshlp.org/content/suppl/2018/06/18/rna.065524.118.DC1
P<P	Published online June 18, 2018 in advance of the print journal.
Accepted Manuscript	Peer-reviewed and accepted for publication but not copyedited or typeset; accepted manuscript is likely to differ from the final, published version.
Open Access	Freely available online through the *RNA* Open Access option.
Creative Commons License	This article, published in *RNA*, is available under a Creative Commons License (Attribution 4.0 International), as described at http://creativecommons.org/licenses/by/4.0/.
Email Alerting Service	Receive free email alerts when new articles cite this article - sign up in the box at the top right corner of the article or **click here.**

Advance online articles have been peer reviewed and accepted for publication but have not yet appeared in the paper journal (edited, typeset versions may be posted when available prior to final publication). Advance online articles are citable and establish publication priority; they are indexed by PubMed from initial publication. Citations to Advance online articles must include the digital object identifier (DOIs) and date of initial publication.

To subscribe to *RNA* go to:
http://rnajournal.cshlp.org/subscriptions